Exhumation Processes in Oceanic and Continental Subduction Contexts: A Review

Stéphane Guillot, Keiko Hattori, Philippe Agard,
Stéphane Schwartz and Olivier Vidal

Abstract Although the exhumation of high pressure (HP) and ultrahigh pressure (UHP) rocks is an integral process in subduction, it is a transient process, likely taking place during the perturbation in subduction zones. Exhumation of HP to UHP rocks requires the weakening of a subduction channel and the decoupling of the exhumed slice from the rest of the slab. Considering more than 60 occurrences of HP to UHP units of Phanerozic ages, we propose three major types of subduction zones:

Accretionary-type subduction zones exhume HP metasedimentary rocks by underplating. The exhumation is slow and can be long-lasting.

The serpentinite-type subduction zones exhume HP to UHP in a 1 to 10 km thick serpentinite subduction channel. The serpentinite matrix originates from both subducted abyssal peridotites and hydated mantle wedge. Exhumation velocity is low to intermediate and the exhumation is driven by the buoyancy and the low-viscosity of the serpentinite.

The continental-type subductions exhume UHP rocks of continental origin. The UHP rocks together with garnet-bearing peridotites form units from km-scale unit. The exhumation is fast, short-lived and occurs at the transition from oceanic subduction to continental subduction. It is driven by buoyancy forces and asthenospheric return flow.

Keywords Oceanic subduction • Continental subduction • Exhumation • HP to UHP rocks • Subduction channel

1 Introduction

Eclogites, HP-LT metamorphic rocks, have been reported since the first petrological description by Haüy (1822) and recognized from many locations in the world with ages ranging from Proterozoic to Phanerozic times (e.g., Godard, 2001 for review). The occurrences of pelitic rocks metamorphosed under eclogite facies conditions suggest that these rocks were subducted to great depths before exhumed (Compagnoni and Maeffo, 1973; Carswell, 1990). The discovery of coesite in Alpine metasediments (Chopin, 1984) introduced the term of UHP metamorphism and demonstrated that continental crust can be subducted to a depth greater than 100–120 km. Most Alpine-type HP to UHP-LT metamorphic rocks occur in peri-Pacific and peri-Mediterranean fold belts of Paleozoic to Tertiary ages (Fig. 1) and are characterized by geothermal gradients ranging between 4 and 10°/km (e.g., Maruyama

S. Guillot
University of Grenoble, OSUG – CNRS,
1381 rue de la Piscine 38041 Grenoble Cedex 9, France,
sguillot@ujf-grenoble.fr

S. Lallemand and F. Funiciello (eds.), *Subduction Zone Geodynamics,*
DOI 10.1007/978-3-540-87974-9,

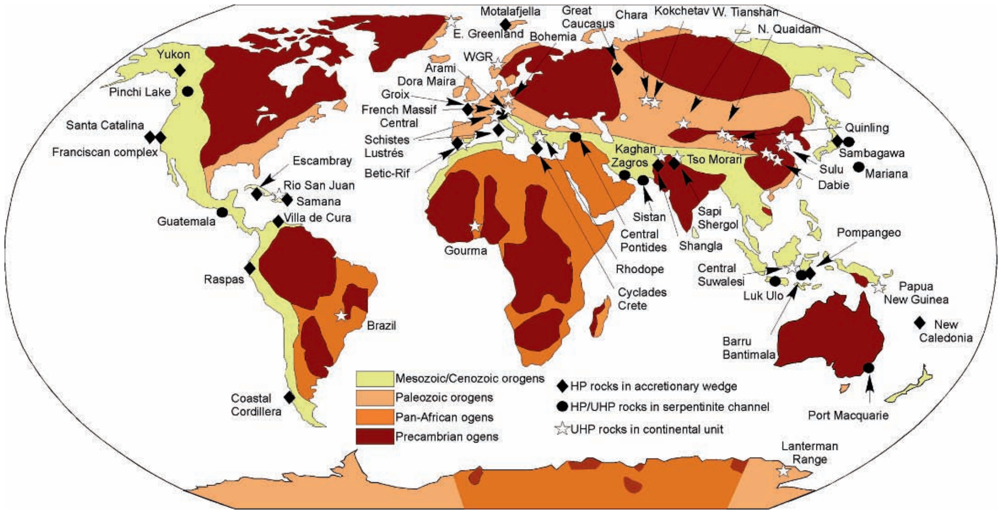

Fig. 1 Worldwide occurrences of HP and UHP massifs (modified after Liou et al., 2004; Tsujimori et al., 2006)

et al., 1996). The oldest UHP unit was described in the Gourma area (eastern Mali) in the Pan-African belt and dated at 620 Ma (Caby, 1994; Jahn et al., 2001). The oldest blueschist is also Late Proterozoic in age (Liou, 1990; Caby et al., 2008). The absence of older blueschists may be ascribed to overprinting by subsequent metamorphism or probably to hotter Earth during Archean and early Proterozoic time. The oldest lawsonite eclogite (e.g., Tsujimori et al., 2006) and oldest carpholite-bearing blueschist (Agard et al., 2005) are both early to middle Paleozoic in age, which is indeed compatible with decreased geothermal gradients to 6–7°/km in Phanerozoic subduction zones (Maruyama et al., 1996). Valli et al. (2004) estimated a geothermal gradient of 30°C/km for a Late Archean subduction zone and Moyen et al. (2006) reported a 3.2 Ga garnet-bearing amphibolite (1.2–1.5 GPa) from an arguably 15°/km subduction zone, similar to those observed during the Late Proterozoic (Maruyama et al., 1996). The oldest reported HP metamorphism (750°C, 1.8 GPa) was found in a 2.0 Ga eclogite terrane of Tanzania (Môller et al., 1995) likely formed as a result of continental subduction (Collins et al., 2004). The peak metamorphic condition indicates a moderate geothermal gradient of about 12°C/km, comparable to geotherms of modern subduction zones. In contrast, the youngest UHP rock on Earth was found in Papua New Guinea and is dated at 4 Ma (Baldwin et al., 2004). These data show that a study of HP to UHP rocks of various ages contributes to a better understanding of the evolution of thermal regimes of subduction zones since Precambrian time.

HP to UHP metamorphic rocks of continental or oceanic origins occur in convergent zones (Ernst, 2001).The pressure-temperature-time (P-T-t) paths suggest their subduction and subsequent return to the Earth's surface (e.g., Duchêne et al., 1997). Despite the growing amount of data on surface horizontal displacement, the vertical movements of the lithosphere and exhumation processes are still in debate. Proposed mechanisms for exhumation include channel flow (Cloos, 1982), corner flow (Platt, 1986), extensional collapse (Dewey et al., 1993), thrusting towards the foreland (Steck et al., 1998), buoyancy assisted by erosion and tectonic processes (Chemenda et al., 1995), compression of a soft zone between two rigid blocks (Thompson et al., 1997), serpentinite channel (Guillot et al., 2001), and coaxial extension associated with a decoupling fault (Jolivet et al., 2003).

Although these mechanisms may locally account for the exhumation of HP to UHP rocks in specific subduction zones, a general understanding of the major processes and associated settings that can explain the worldwide exhumation of HP to UHP rocks is still missing.

Detailed studies of HP and UHP rocks including kinematic analyses and dating of metamorphism provide invaluable information of thermomechanical processes in subduction zones (Coleman, 1971; Ernst, 1973). Such information can also constrain possible mechanisms of exhumation because different processes result in different styles of deformation and P-T-t paths of exhumed rocks. Furthermore, the data from HP and UHP rocks in conjunction with P-T-t paths predicted from numerical modelling provide key information related to the thermomechanical properties of subduction zones.

This paper reviews more than 60 occurrences of HP to UHP units of Phanerozic ages (Fig. 1), their protoliths, their P-T-t paths and their exhumation rates, and discusses the important factors controlling their exhumation and the possible significance of the so-called "subduction channel" in subduction zones.

1.1 Subduction Types

Bally (1981) defined two contrasting types of convergent zones: the Pacific- and Alpine-types. The Pacific-type subduction is characterized by long-lasting subduction of oceanic lithosphere. The Alpine-type first involves the consumption of an oceanic domain, similar to the Pacific-type subduction, followed by the subduction of continental margins. The continents involve in the Alpine-type could be large, such as those in the Alps, Variscides, Himalaya, Dabieshan or the Caledonides (Chopin, 1984; Lardeaux et al., 2001; Guillot et al., 2003, Yang et al., 2003; Hacker, 2007). Some continents are small, as those in Aegean (Jolivet et al., 2003) and Kazakstan (Hacker et al., 2003). Based on the the lithology, the peak P-T conditions, and the exhumation patterns of metamorphic rocks, we propose three types of dominant subduction regime to explain the different styles of exhumation observed: the accretionary-type, the serpentinite-type and the continental-type. The continental-type is similar to the Alpine-type defined by Bally (1981). A subduction zone may evolve from one type to others during its life and two different types may co-exist along one subduction zone.

1.2 Accretionary-Type Subduction

Forearc accretionary wedges (or prisms) develop in front of intra-oceanic arcs or continental arcs (Fig. 2). They are observed all along the Pacific subduction systems including the west coast of the North America (Alaskan–Cascades), the west coast of the South American (Ecuador-Chile), Japan, and Suwalesi. They also occur in the Barbados in the western Atlantic Ocean and Makran in the northern Indian Ocean (e.g., Lallemand, 1999). A major feature of accretionary wedges is the stacking of oceanic sediments by offscraping of the upper part of subducting plate or arc rocks eroded from the upper plate depending on the geometry of the buttress and the subduction angle (Cloos, 1982; Platt, 1986; Moore and Silver, 1987; Cloos and Shreve, 1988; Von Huene and Scholl, 1991)

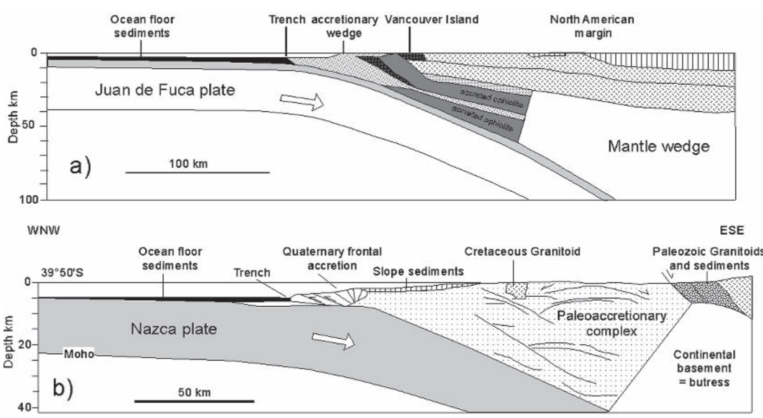

Fig. 2 (**a**) Schematic cross section through the Cascadia subduction zone beneath the Vancouver Island (modified after Hyndman, 1995). Note that the deep part of the accretionary wedge is comprised of imbricate slices of ophiolites and sediments. (**b**) Schematic cross section through the South-Central Chilean forearc based on reflection seismic data and offshore geology (modified after Glodny et al., 2005). Note that the paleoaccretionary wedge of Upper Paleozoic age show internal structures compatible with underthrusting at the base and extension at shallow level. Upper Paleozoic blueschists (~0.8 GPa) are being exhumed near the toe of the paleoaccretionary wedge

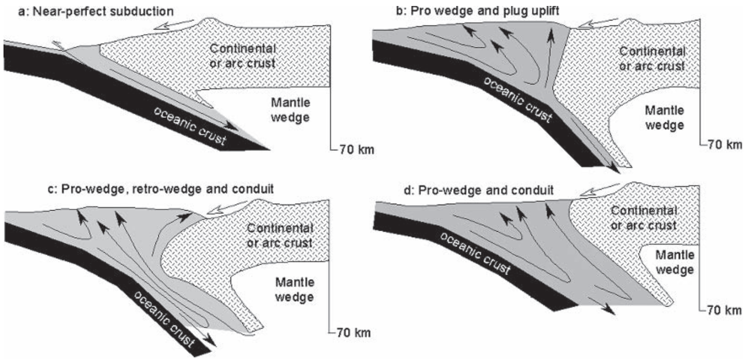

Fig. 3 Schematic geometry of accretionary prism (modified after Ernst, 2005). Note that the geometry controls the depth and origin of HP rocks either from upper or lower plates, and the exhumation trajectory. (**a**) In a narrow accretionary prism, a slab is parallel to the buttress, which prevents the exhumation of HP rocks. (**b**) In a wide accretionary wedge at shallow depth, the rocks are exhumed only from shallow depth. (**c**) In an intermediate model where an accretionary prism is wider than that in Fig. 3b, but narrower than that in Fig. 3d. (**d**) An accretionary wedge is wide at shallow and deep levels, which allow the exhumation of HP rocks from great depths at front, middle and rear of the wedge

(Fig. 3). The deepest part of an accretionary wedge is close to the buttress and about 20 km (ca. 0.6 GPa) in present-day subduction zones, but in exceptional cases about 40–60 km (1.1–1.6 GPa) in Chile (Glodny et al., 2005) and Cascadia beneath Vancouver Island (Hyndman, 1995) (Fig. 2).

Numerical simulation of an accretionary wedge (Beaumont et al., 1999; Allemand and Lardeaux, 1997; Yamato et al., 2007) shows that the initial geometry of a buttress or backstop (continental crust for active margin and arc crust for intra-oceanic subduction) affects the shape of an accretionary wedge and consequently the metamorphic pressures reached by the exhumed rocks. When a slab is parallel to a buttress, deeply subducted rocks are prevented from exhumation (Fig. 3a). On the other hand, a wide open wedge allows the exhumation of deeply subducted rocks that originated from the upper and lower plates (Fig. 3d). In intermediate geometries, deeply subducted rocks are exhumed close to the trench (pro-wedge exhumation), vertically (plug uplift) and also near the buttress (retro-wedge exhumation) (Ernst, 2005).

The geometries shown in Fig. 3b, c are conducive for the exhumation of HP rocks during active oceanic subduction. As already discussed, accretionary wedges are dominated by sediments derived from the upper and lower plates and contain exhumed HP-LT rocks. Two recent reviews by Tsujimori et al. (2006) and Agard et al. (submitted) list more than 20 HP and UHP massifs in the world belonging to this category (Table 1). All these units share many features, suggesting that similar processes were in operation during their metamorphism and exhumation of the HP rocks. These features are summarized below.

The HP-LT rocks in accretionary-type subduction zones are dominated by clastic sedimentary rocks with no mantle-derived material, suggesting that the protoliths of HP-LT rocks are sediments deposited on the sea floor and that the detritus of the sediments were supplied from the upper and lower plates (Plate 1a, Fig. 4a). For instance, upper crustal rocks of seamounts underwent HP-LT metamorphism in the Himalaya (e.g., Mahéo et al., 2006). The HP-LT unit in the Himalaya also contains arc-derived material, suggesting that the erosion of arc rocks was contemporaneous during the seamount subduction (e.g., Lallemand and Le Pichon, 1987; Von Huene and Cullota, 1989; Mahéo et al., 2006). The exhumation of only upper crustal rocks implies that lower crustal rocks of slabs are deeply subducted.

The relative abundance of oceanic sediments and upper oceanic crust in exhumed rocks varies from one subduction zone to another. Centimetric to hectometric blocks of mafic or ultramafic oceanic rocks is usually observed in a calcsilicate matrix. In the case of the Franciscan complex, this "melange" was previously interpreted as a tectonic melange developed along the subduction zone, leading to the concept of subduction channel where a soft matrix allows rigid blocks to be exhumed parallel to the subduction plane (Cloos, 1982;

Table 1 Compilation of available data on exhumed high pressure rocks in accretionary wedge

Unit	Samana Peninsula Dominican Republic	Escambray Cuba	Schistes Lustrés Corsica	Schistes Lustrés Western Alps	Franciscan C. California	Santa Catalina California	Coastal Cordillera Chile	Pam Peninsula New Caledonia	Motalafjella Spitsbergen	Shangla Pakistan	Groix France
Abbreviation	SA	ES	SLC	SLA	FC	SC	CC	PP	MS	SP	GX
Subduction context	Intra-oceanic	Intra-oceanic	Intra-oceanic	Intra-oceanic	Intra-oceanic	Intra-oceanic	Active margin	Intra-oceanic	Unknow	Intra-oceanic	Intra-oceanic
Tectonics of exhumed rocks	3 nappes	3 nappes	3 nappes	4 nappes	Several nappes	3 nappes	Sevreal nappes	>2 nappes	2 nappes	3 nappes	2 nappes
Lithology of exhumed rocks	Sedimentary rocks with serp and basic lenses	Sedimentary rocks with serp and basic lenses	Ophiolitic rocks with sedimentary cover	Sedimentary rocks with serpentinites and basic lenses	Ophiolitic rocks with sedimentary cover	Ophiolitic rocks with sedimentary cover	Sedimentary rocks with basic lenses	Ophiolitic rocks with sedimentary cover	Sedimentary rocks with basic lenses	Sedimentary and volcanic melange	Sedimentary rocks with basic lenses
Max P-T conditions	2.2–2.4 GPa	1.6–2.3 GPa	2.0 GPa	1.8–2.0 GPa	1.8–2.2 GPa	1.2 Gpa	1.1–1.6 GPa	2.0 GPa	1.8–2.4 GPa	0.7 Gpa	1.6–2.0 GPa
	610–625°C	530–620°C	390°C	500°C	360–445°C	600°C	600–760°C	460°C	580–640°C	400°C	500°C
Metamorphic age	Cretaceous-Eocene	Cretaceous-Eocene	Cretaceous-Eocene	Cretaceous-Eocene	Middle Jurassic	Cretaceous	Carboniferous	Eocene	Ordovician	Cretaceous	Devonian
Exhumation velocities	~1 mm/year	Unknown	<2 mm/year	<2 mm/year	5 mm/year	<2 mm/year	0.6 mm/yr	2–3 mm/year	Unknown	Unknown	2 mm/year
Exhumation timing	When the accretionary wedge collided	When the accretionary wedge collided	Intra-oceanic	Intra-oceanic	Intra-oceanic	Intra-oceanic	Active subduction	When the accretionary wedge collided	Unknown	Intra-oceanic	When the accretionary wedge collided
References	Goncalvez et al., 2000	Schneider et al., 2004	Caron and Péquignot, 1986	Agard et al., 2002	Platt, 1986	Bebout and Barton, 1993	Willner et al., 2004	Cluzel et al., 2001	Hirajima et al., 1988	Jan, 1985	Bosse et al., 2005
	Zack et al., 2004	Stanek et al., 2006		Tricart and Schwartz, 2007	Oh and Liou, 1990	Sorensen, 1988	Glodny et al., 2005	Fitzherbert et al., 2005	Agard et al., 2005	Anczkiewicz et al., 2000	
	Escuder-Viruete and Pérez-Estaùn, 2006					Anczkiewicz et al., 2004					

(continued)

Table 1 (continued)

Unit	Sapi-Shergol India	Sanbagawa Japan	Raspas Ecuador	Gourma Mali	Villa de Cura Venezuela	Pompangeo Suwalesi	Betic-Rif-Tell Spain-Morocco-Canada	Yukon	Great Caucasus Russia	Cyclades Greece	Crete
Abbreviation	SS	SJ	RE	GM	VC	PS	BRT	YC	GC	CG	C
Subduction context	Intra-oceanic	Intra-oceanic	Active margin	Active margin	Intra-oceanic	Intra-oceanic	Intra-oceanic	Active margin	Active margin	Intra-oceanic	Intra-oceanic
Tectonics of exhumed rocks	2 nappes	3 nappes	3 nappes	3 nappes	4 nappes	2 nappes	3 nappes	several nappes	3 nappes	4–6 nappes	
Unit	Samana Peninsula Dominican Republic	Escambray Cuba	Schistes Lustrés Corsica	Schistes Lustrés Western Alps	Franciscan C. California	Santa Catalina California	Coastal Cordillera Chile	Pam Peninsula New Caledonia	Motalafjella Spitsbergen	Shangla Pakistan	Groix France
Lithology of exhumed rocks	Sedimentary and volcanic melange	Sedimentary rocks with magmatic rocks	Ophiolitic rocks with sedimentary cover	Sedimentary rocks with volcanic rocks	Ophiolitic rocks	Sedimentary rocks with volcanic rocks	Sedimentary rocks	Ophiolitic rocks with sedimentary cover	Continental units	Sedimentary rocks	Sedimentary rocks
Max P-T conditions	0.9–1.0 GPa	2.0–2.1 GPa	1.9–2.0 GPa	1.6 GPa	0.8 GPa	1.2 GPa	1.8–2.0 GPa	1.5 GPa	1.6 GPa	2.0 GPa	1.6 GPa
	350–420°C	600°C	530–630°C	550–650°C	375°C	450°C	550–650°C	420–650°C	620–700°C	500°C	400°C
Metamorphic age	Cretaceous	Early Cretaceous	Cretaceous	Pan-African	Cretaceous	Cretaceous	Cretaceous-Paleocene	Carboniferous-Triassic	Devonian	Eocene	Miocene
Exhumation velocities	Unknow	<1 mm/year	2.5–5 mm/year	Unknown	Unknown	Unknown	2.8 mm/year	Unknown	~4 mm/year	2.6 mm/year	~5 mm/year
Exhumation timing	Intra-oceanic	Early stage of subduction	Active subduction	Unknown	Intra-oceanic	When the accre-tionary wedge collided	Intra-oceanic with slab retreat	When the accretionary wedge collided	When the accretionary wedge collided	Intra-oceanic with slab retreat	Intra-oceanic with slab retreat
References	Honegger et al., 1989	Wallis et al., 2004	Arculus et al., 1999	Caby et al., 2008	Avé Lallemant et al., 2005	Parkinson et al., 1998	Platt and Vissers, 1989	Erdmer et al., 1998	Perchuk and Philippot, 1997	Jolivet et al., 2003	Jolivet et al., 2003
	Mahéo et al., 2006	Ko et al., 2005	Gabriele et al., 2003				Augier et al., 2005	Philippot et al., 2001		Forster and Lister, 2005	
		Ota et al., 2004									

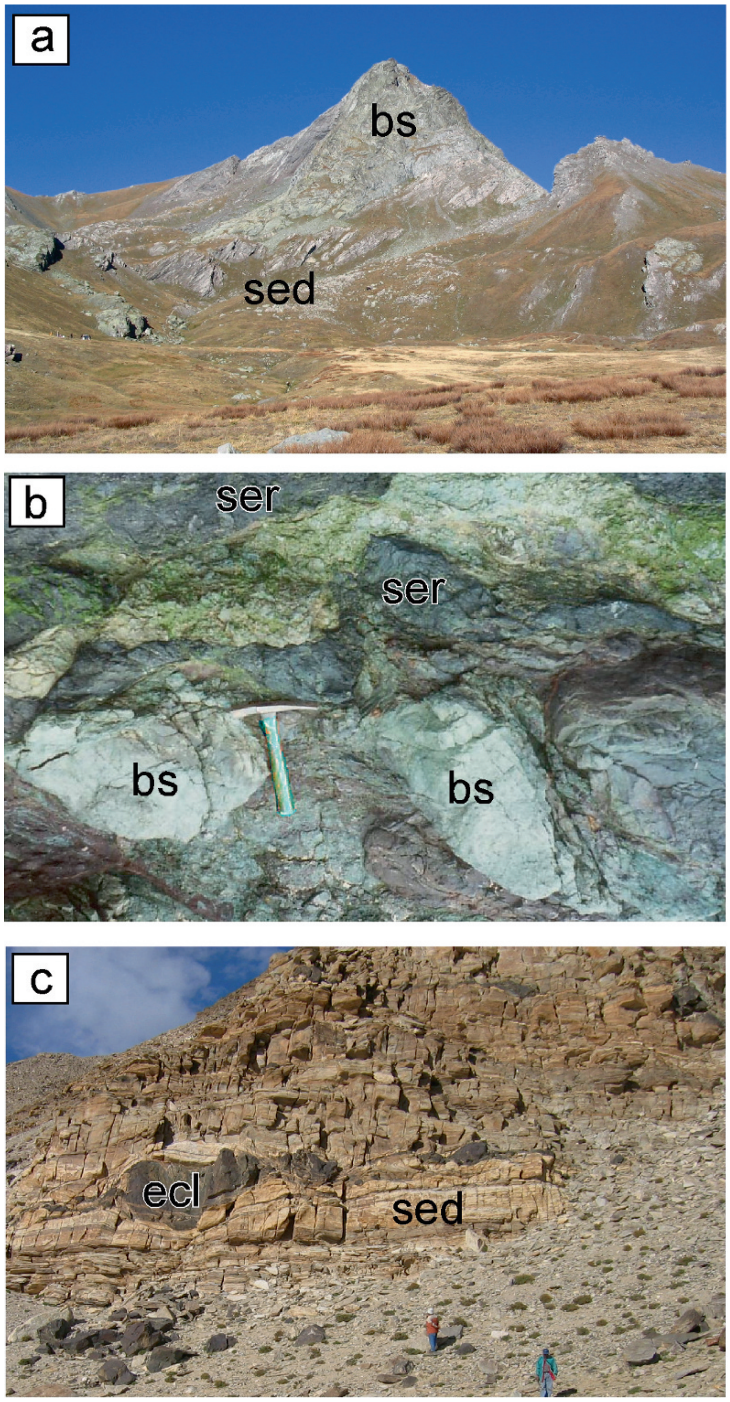

Plate 1 Field photographs of HP rocks in three subduction types. (**a**) Accretionary type subduction. Block of an hectometric blueschist (bs) corresponding to an oceanic olistolith embedded in a metasediemnatry matrix (sed) of Schistes Lustrés at Bric Bouchet, Queyras in western Alps. The contact between the blueschist and the metasediment is concordant and both recorded similar P-T conditions. (**b**) Serpentinite type. Metric blocks of blueschists (bs) of oceanic origin are embedded in a serpentinite matrix (ser). At the local and regional scale, each blueschist block recorded different peak metamorphic conditions in Northern Serpentinite mélange in Cuba. (**c**) Continental subduction context. Coesite-bearing eclogitic block (ecl) corresponding initially to a basaltic dyke emplaced in Permian sediment (sed) on the Indian continental margin. The intrusive contact between the dyke and sediments is preserved at the regional scale, and the Indian continental margin forms a coherent UHP unit of 100 *50 km at Tso Morari in western Himalaya

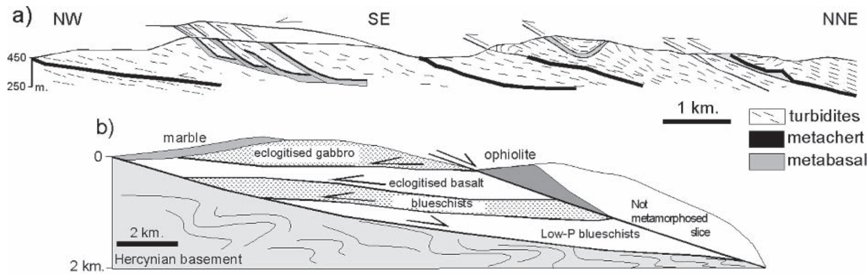

Fig. 4 (**a**) Nappes observed in the HP Franciscan complex. Note that the primary sedimentary contact between basalts and chert is preserved (modified after Kimura et al., 1996). (**b**) Schematic succession of HP nappes in the Cycladic blueschist belt in Greece (modified after Forster and Lister, 2005)

Shreve and Cloos, 1986). Ocean Drilling Project in the 80's documented that gabbros and dolerites are brecciated near ridges (Lagabrielle et al. 1981; Lagabrielle and Polino, 1985) (Plate 1a) and that breccias and olistoliths form by mixing of igneous rocks and sediments on the sea floor. Earlier, mineralogical studies suggested that lower metamorphic grade of the matrix than mafic lenses, but this interpretation has been questioned by recent studies showing that the matrix metasediments and lenses record similar P-T conditions (e.g., Kimura et al., 1996 for the Franciscan complex; Agard et al., 2002 for the Western Alps; Parra et al., 2002 for the Cyclades in Greece).

In term of geometry, several units are recognized in exhumed rocks with a thickness varying from the hectometre up to 5 km (e.g., two to four units in Kimura et al., 1996; Stanek et al., 2006). These units form nappes thrust towards the paleo-trench with lower metamorphic units overlain by higher metamorphic units (Fig. 4a). These nappes started to develop under HP-LT conditions, generally under blueschist conditions and ended under greenschist facies conditions, suggesting that the early exhumation is accommodated by thrusting (Fig. 4). Late extension that starts at the ductile-brittle transition commonly affects the nappes as documented in the Franciscan complex (Platt, 1986), the Samana complex in Dominican Republic (Goncalvez et al., 2000), the Cyclades in Greece (Jolivet et al., 2003) and the Piedmont complex in the western Alps (Tricart et al., 2004).

The maximum pressures recorded in exhumed rocks vary from 0.7 to 2.0 GPa and plot along geotherms ranging between 5 and 14°/km, which are similar to those of modern subduction zones (Fig. 5). Several eclogites show pressures equivalent to a depth of about 75 km. This is much deeper than the maximum depth, 20–40 km, observed in most active accretionary wedges. Another common feature of HP-LT rocks is slow exhumation rates ranging between 1 and 5 mm/year (Table 1), which are independent of subduction velocities (e.g., Agard et al., submitted).

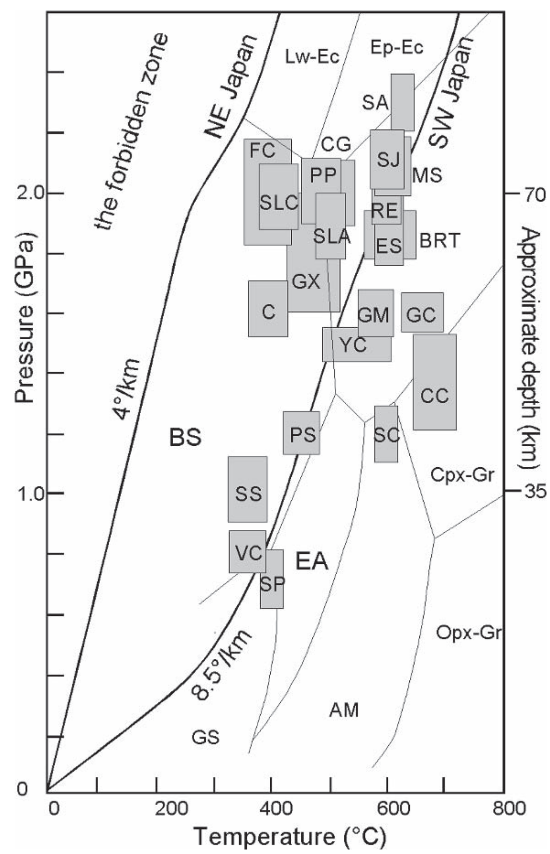

Fig. 5 Compilation of P-T data for accretionary wedge context (see Table 1 for abbreviations and references). Cold (4°/km, NE Japan) and hot (8.5°/km, SW Japan) geotherms from Peacock and Wang (1999). Lx-Ec: lawsonite eclogite; Ep-Ec: epidote eclogite; *Am-Ec* amphibole eclogite, *BS* blueschist, *Cpx-Gr* clinopyroxene granulite, *Opx-Gr* orthopyroxene granulite, *EA* epidote amphibolite, *AM* amphibolite, *GS* greenschist

1.3 The Serpentinite-Subduction Channel

Recent petrological and geophysical evidence documented the presence of serpentinites in oceanic floor (e.g., Mével, 2003) and along active subduction zones (e.g., Furukawa, 1993; Maekawa et al., 1993; Bostock et al., 2002; Seno and Yamasaki, 2003). Serpentine minerals sensus lato display several distinctive characters: they contain up to 13 wt% of water and can be a major host of fluid-mobile elements in deep subduction zones (e.g., Schmidt and Poli, 1998; Hattori and Guillot, 2007) as they are stable under wide temperatures and pressures down to a depth of 150–170 km (Ulmer and Trommsdorff, 1995). They have a low density, about 2600 kg/m^3, a low viscosity of about 4.10^{19} Pas, a high poisson ratio (0.29) and low shear modulus (e.g., Moore and Lockner, 2007; Reynard et al., 2007; Hilairet et al., 2007). These physical properties allow serpentinites to be highly ductile to lubricate subduction planes (Guillot et al., 2001).

In paleo-subduction zones, serpentinites are commonly associated with HP-LT rocks and have been considered as fragments of oceanic lithosphere, and the contacts between eclogitic lenses and the matrix serpentinites are interpreted to be primary (e.g., Coleman, 1971). For instance, the high-pressure Monviso massif in the Western Alps has been considered as a continuous sequence of the Tethyan oceanic lithosphere (ophiolite). However, recent studies show that this massif represents a deep tectonic melange as individual eclogitic blocks record different P-T conditions (Fig. 6a) (Blake et al., 1995; Schwartz et al., 2000, 2001). Sixteen Phanerozic massifs are defined as serpentinite-type subduction complexes (Table 2). The Zermatt-Saas unit is included in this type because mafic bodies are intimately associated with serpentinites, although it is not a tectonic melange and has been interpreted as a complete ophiolite sequence (e.g., Li et al., 2004).

HP-LT units exhumed in serpentinite-type subduction zones are dominated by highly sheared serpentinites that contain blocks of metabasites (Plate 1b). The blocks are weakly deformed and range in size from metric to decametric. Some blocks are kilometric, as those in the Monviso massif, or centimetric, as those in the Voltri massif. The metasediments (metacherts, metagreywackes, metapelites, marbles) are highly deformed and minor in volume, less than 10% of the massifs (Fig. 6b).

The initial geometry is difficult to reconstruct because original contacts are no longer recognized in exhumed rocks. Nevertheless, it has been evaluated in two well studied locations; the Monviso and Voltri massifs in the Alps (Fig. 6). The Monviso massif is composed of six west-dipping tectono-metamorphic units of metabasalts and metagabbroic rocks, each of which is separated by west dipping normal shear zones containing serpentinites (Lombardo et al., 1978; Schwartz et al., 2000; Guillot et al., 2004; Fig. 6a). The basal unit is serpentinites with 400 m in thickness. The serpentinites that originated from lherzolite and minor harzburgite and dunite, are cut by sheared dykes of rodingitized gabbro and basalt. The serpentinite layer commonly contains metric to hectometric lenses of foliated eclogitic gabbro, ferrogabbro and metamorphosed plagiogranite. Considering the geometry, this basal serpentinite unit likely had an initial size of about 50 km × 10 km (Schwartz et al., 2001; Guillot et al., 2004). Five other units are composed of discontinuous layers of intensely deformed and recrystallized metagabbros. These metagabbros contain minor ultramafic cumulates and hydrated mantle peridotites (Messiga et al., 1999). Locally, greenschists and banded glaucophane-epidote metabasalts retain the pillow lava texture. The upper part of the massif exposes thin layers of carbonate-bearing micaschists (Schistes Lustrés) interbedded with the metabasites. The thickest section (~1.2 km) is composed of basalt breccia, pillow lavas, metagabbro and slices of serpentinites in upward direction. The serpentinites were metamorphosed under blueschist facies conditions. The Monviso massif is thus similar to a dismembered ophiolitic massif, yet each unit records different P-T conditions.

The Voltri massif in the western Alps is more akin to a mélange zone observed in British Columbia (Tsujimori et al., 2006) Cuba (Garcia-Casco et al., 2002), Dominican Republic (Krebs et al., 2008), and Turkey (Altherr et al., 2004). It is surrounded by highly sheared serpentinites and consists of chaotic mixture of meter-sized blocks of metagabbros, metabasites, métasediments and also serpentinites in the matrix of schistose chlorite-actinolite (Fig. 6b) (Vignaroli et al., 2005; Frederico et al., 2007). The serpentinte matrix both in the Monviso and Voltri massifs record HP conditions (Auzende et al., 2006).

Geochemical and petrological data suggest that mafic blocks in 18 serpentinite-type subduction complexes were derived from the subducted oceanic plate

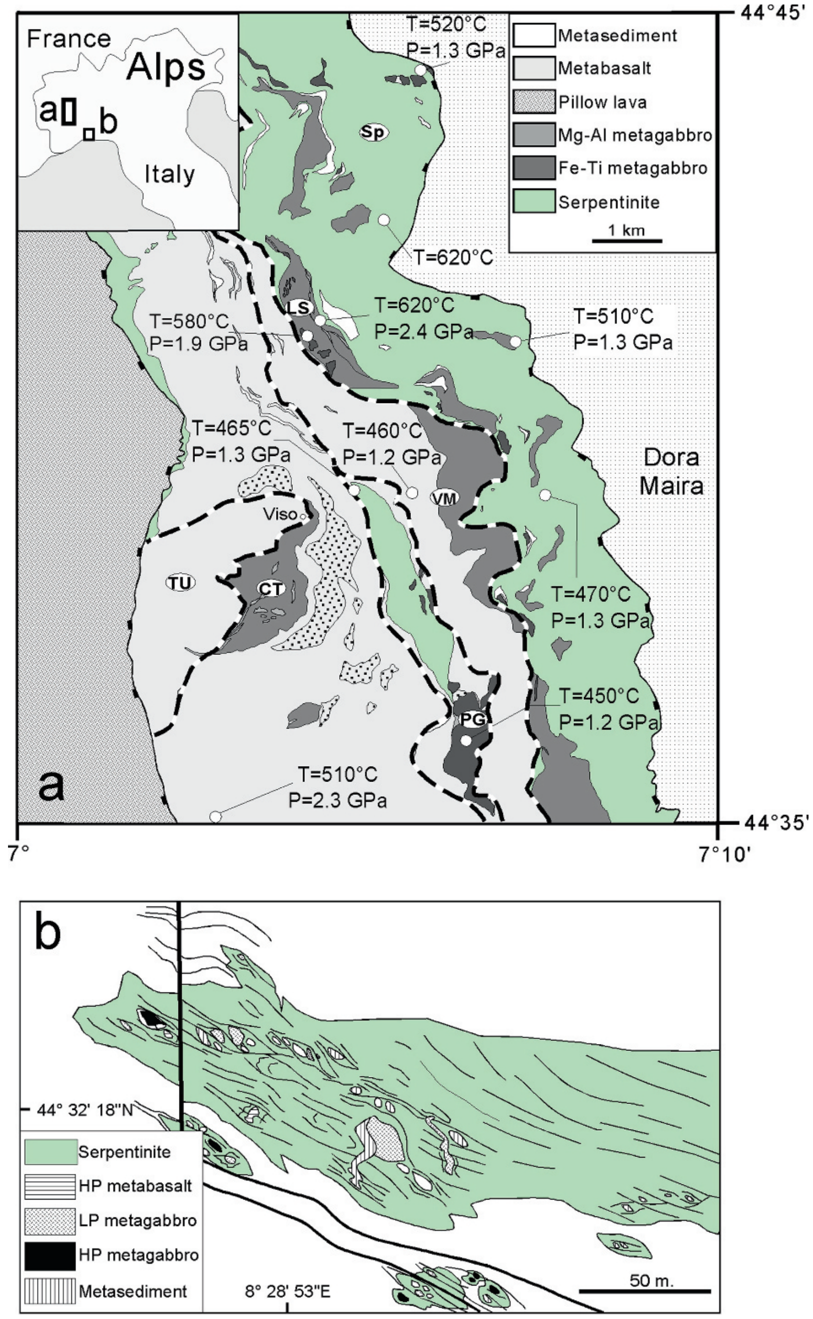

Fig. 6 (**a**) Lithological map of the central part of the Monviso in Western Alps (after Schwartz et al., 2001). At the regional scale, a network of normal shear zone underline by sheared serpentinites or sheared metasediments separated several metabasite blocks recording contrasted P-T conditions. The basal serpentinites unit (on the right side) forms a thick (400 m) serpentinite melange containing metric blocks of metabasalts, metagabbros of metasediments. *CT*: Costa Ticino; *PG*: Passo Galarino; *LS*: Lago Superiore; *TU*: Tour Real; *VM*: Viso Mozzo; *SP*: Basal Serpentinite; *TU*: (**b**) Geological and structural map of the Erro Tobio serpentine mélange (Southwestern Alps). Note the diversity of lithologies included in the serpentinite matrix (modified after Frederico et al., 2007)

Table 2 Compilation of available data on exhumed high pressure rocks in serpentinite subduction channel

Unit	South Motagua Guatemala	Central Pontides Turkey	Port Macquarie Australia	Pinchi Lake Canada	Barru Complex Suwalesi	Bantimala Complex Suwalesi	Luk Ulo Java	Zagros Iran	Sistan Iran
Abbreviation	SM	CP	PM	PL	BC	BAC	LU	ZA	SI
Subduction context	Intra-oceanic	Intra-oceanic	Intra-oceanic	Unknown	Active margin	Active margin	Active margin	Active margin	Active margin
Tectonics	Tectonic block within serpentinite melange	Tectonic block within serpentinite melange	Tectonic block within serpentinite melange	Tectonic block within serpentinite melange	Tectonic block within serpentinite melange	Tectonic block within serpentinite melange	Tectonic block within serpentinite melange	Tectonic block within serpentinite melange	Tectonic block within serpentinite melange
Lithology of exhumed rocks	Serpentinites, mafic rocks Metsediments	Serpentinites, mafic rocks	Serpentinites, mafic rocks	Serpentinites, mafic rocks	Serpentinite Metasediments	Serpentinites, mafic rocks Metsediments	Serpentinites, mafic rocks Metsediments	Serpentinites, mafic rocks Volcanoclastics	Serpentinites, mafic rocks Volcanoclastics
Protoliths of mafic rocks	MORB	MORB	MORB	MORB	MORB	MORB	MORB	MORB	MORB
Protoliths of serpentinites	Unknown	Probably mantle wedge	Mantle wedge	Unknown	Unknown	Unknown	Oceanic	Oceanic	Oceanic
Max P-T conditions	2.5 GPa 470°C	P > 1.4 GPa 400–430°C	2.0–2.4 GPa 420–570°C	2.2 GPa 450°C	2.1 GPa 520°C	2.4–2.7 GPa 580–620°C	2.2 GPa 365°C	1.8 GPa 500°C	1.9–2.2 GPa 600°C
Metamorphic age	Cretaceous	Cretaceous	Cretaceous	Triassic	Cretaceous	Cretaceous	Cretaceous	Cretaceous	Cretaceous
Exhumation velocities	~4 mm/yr	Unknown	Unknown	Unknown	Unknown	Unknown	Unknown	2–3 mm/year	Unknown
Exhumation timing	When the subduction melange collided with continent	Unknown	Intra-oceanic associated with change in stress field	Unknown	When the subduction melange collided with continent	When the subduction melange collided with continent	When the subduction melange collided with continent	Intra-oceanic change in subduction with rate	Intra-oceanic
References	Harlow et al., 2004 Tsujimori et al., 2006	Altherr et al., 2004	Aitchinson et al., 1994 Och et al., 2003	Ghent et al., 1993 Tsujimori et al., 2006	Parkinson et al., 1998	Parkinson et al., 1998	Kadarusman et al., 2007	Agard et al., 2006	Fotoohi Rad et al., 2005

(*continued*)

Table 2 (continued)

Rio San Juan Dominican Republic	Zaza Cuba	Monviso Italy	Zermatt Switzerland	Voltri Italy	Mariana	Omachi Izu Bonin	Borus-Chagan-Uzun Gorny Altai	Chara and Maksyutov Kazkhstan-Urals	Higashi-Akaishi Sanbagawa Japan
RSJ	ZZ	MV	ZS	VO	MA	OM	BCU	CM	SAJ
Intra-oceanic	Intra-oceanic	Intra-oceanic	Intra-oceanic	Intra-oceanic	Intra-oceanic	Intra-oceanic	Intra-oceanic	Intra-oceanic	Continental margin
Tectonic block within serpentinite melange	Tectonic block within serpentinite melange	Tectonic block within serpentinite melange	Coherent ophiolitic unit	Tectonic block within serpentinite melange	tectonic block within mud volcanoes	Tectonic block within serpentinite melange	Tectonic block within serpentinite melange	Tectonic block within serpentinite melange	Tectonic block within serpentinite melange
Peridotites serpentinites amphibolitic rocks	Serpentinites, mafic rocks	Serpentinites, mafic rocks metsediments	Serpentinites, mafic rocks metsediments	Serpentinites, mafic rocks metsediments	Serpentinites, mafic rocks	Serpentinites, mafic rocks	Serpentinites, mafic rocks metsediments	Serpentinites, mafic rocks metsediments	Peridotites serpentinites amphibolitic rocks
MORB	MORB	MORB	MORB	MORB	MORB	Andesite	MORB OIB	MORB OIB	MORB
Mantle wdege	Mantle wedge and oceanic	Oceanic	Oceanic	Oceanic	Mantle wedge	Mantle wedge	Oceanic & mantle wedge	Oceanic & mantle wedge	Mantle wedge
4.0 GPa	2.0 GPa	2.6 GPa	2.8 GPa	2.2 GPa	0.7 GPa	2.0 GPa	2.0 GPa	eclogites	3.8 GPa
1550°C	600°C	630°C	600°C	550°C	150–250°C	~650°C	660°C		810°C
Cretaceous	Cretaceous	Eocene	Eocene	Eocene	Present-day	Oligocene	Cambrian	Silurian	Early Cretaceous
~6 mm/year	Unknown	~10 mm/year	~10 mm/year	3–4 mm/year	Unknown	Unknown	Unknown	Unknown	Unknown
When the subduction melange collided with continent	When the subduction melange collided with continent	When the subduction melange collided with continent	When the subduction melange collided with continent	When the subduction melange collided with continent	Intra-oceanic	Intra-oceanic with back-arc extension	When the subduction melange collided with continent	When the subduction melange collided with continent	Syn-subduction
Abbott et al., 2006	Garcia-Casco et al., 2002	Blake et al., 1995	Reinecke, 1991	Hermann et al., 2000	Maekawa et al., 1993	Ueda et al., 2004	Dobretsov and Buslov, 2004	Dobretsov and Buslov, 2004	Enami et al., 2004
	Hattori and Guillot, 2007	Schwartz et al., 2000	Li et al., 2004	Frederico et al., 2007	Fryer et al., 1999				

(Table 2). The possible exception is the eclogitic blocks of andesite origin dredged near the Omachi forearc serpentinite diapir (Izu-Bonin arc) (Ueda et al., 2004).

Serpentinites in oceanic subduction zones mostly originated from abyssal peridotites and their hydration likely took place during the ridge hydrothermal activity, such as those in Java, Iran, and the Alps. Some serpentinites were derived from hydrated mantle wedges (Turkey, Australia, Mariana, Izu-Bonin) or both (Northern serpentinite mélange in Cuba and Dominican Republic) (Table 2).

Regarding the metamorphic conditions, most eclogitic blocks reached HP between 1.8 and 2.5 GPa and relatively low temperatures, which defines paleogeothermal gradients lower than 10°C/km (Fig. 7). Two localities provide evidence for deeper P-T conditions, at 3.2 and 4 GPa, respectively (SAJ, RSJ; Table 2; Fig. 7), as deduced from garnet peridotite blocks embedded in the serpentinite melange.

In the Western Alps and in the northern serpentinite mélange in the Dominican Republic, the maximum pressure of each block varies from 1.0 to 2.3 GPa (Schwartz et al., 2000; Frederico et al., 2007; Krebs et al., 2008), suggesting that their juxtaposition unlikely took place during exhumation. The metamorphic ages of different blocks show ranges in age; ±4 Ma in the Voltri massif in the western Alps (Frederico et al., 2007), ±15 Ma in the Monviso massif (e.g., Guillot et al., 2004) and 40 Ma in the Rio San Juan complex in Dominican Republic (Krebs et al., 2008). These variations likely reflect different depths and different times of metamorphism for blueschists or eclogitic blocks within the subduction channel. Finally exhumation velocities vary between 3 and 10 mm/year, which are faster than those recorded in accretionary wedge environment (Table 2). Again the exhumation velocity remains independent of the subduction velocity (e.g., Agard et al., submitted for publication).

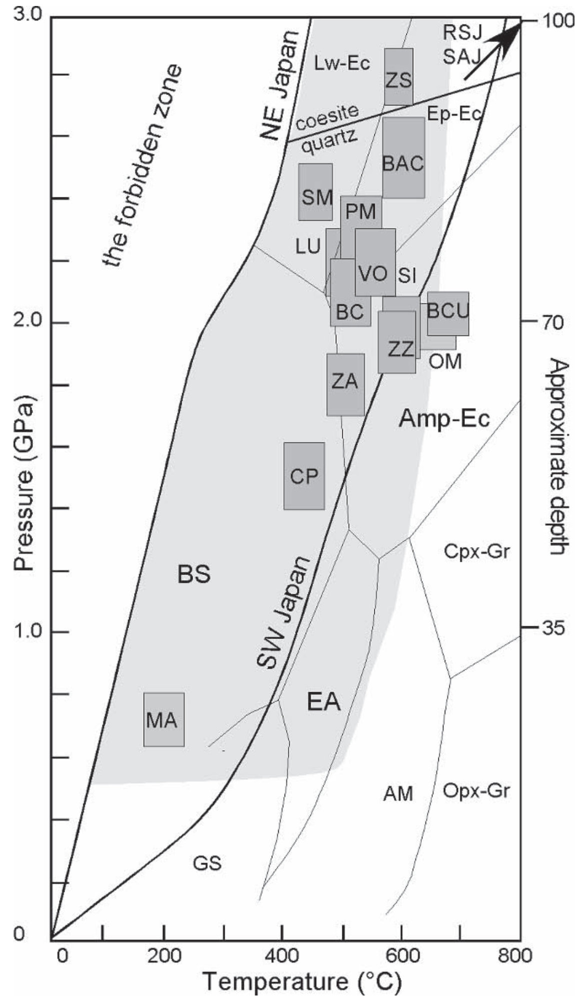

Fig. 7 Compilation of P-T data for serpentinite subduction channel context (see Table 2 and Fig. 5 for abbreviations and references). Grey area: stability field of antigorite after Ulmer and Trommsdorff (1995)

1.4 Continental-type Subduction

The discovery of coesite and microdiamond in subducted crustal rocks (Chopin, 1984; Smith, 1984; Sobolev and Shatsky, 1990) demonstrated that continental rocks can be subducted to depths of at least 100 km. Such UHP rocks have now been documented in most Phanerozoic mountain belts around the world (Fig. 1) but the mechanism by which these rocks were exhumed are still debated. This problem is not trivial because of the large sizes of some HP-UHP terranes (>50,000 km^2 in China and Norway), the large vertical displacement during their exhumation and the preservation of index minerals or assemblage (Grasemann et al., 1998; Hacker, 2007).

The protoliths of UHP rocks are predominantly upper continental crust (Table 3), such as granite gneisses, and metasedimentary rocks (quartzites, metapelites, and marbles). Mafic plutonic rocks are present in subduction zones, but they correspond to

Table 3 Compilation of available data on exhumed UHP rocks in continental and oceanic subduction complexes

Massif	Rhodope Greece	Ulten zone peridotites Italie, Alps	Dora Maira Italie	Alpes Arami Switzerland	d'Entrecasteaux Papua New Guinea	Lanterman Range Antarctica	North Quinlin-Dabie-Sulu China	South Quilin-Dabie China	Tianshan China	Kokchetav
Abbreviation	Rh	UZ	DM	AA	EN	LR	NQDS	SQD	TIA	KO
Subduction context	Microcontinent subduction	Continental subduction	Continental margin subduction	Continental subdcution	Continental margin subduction	Continental margin subduction	Continental margin subduction	Continental margin subduction	Continental subdcution	Microcontinent subduction
Tectonics	4 nappes	3 nappes	3 nappes	Several nappes	Metam. core complex	3 nappes	>3 nappes	<3 nappes	4 nappes	Several nappes
Lithology	Continental rocks with oceanic rocks	Garnet peridotites within gneiss and migmatites	Peridotites, felsic amphibolitic rocks	Peridotites, felsic amphibolitic rocks	Mafic lenses within gneisses		Peridotites, felsic amphibolitic rocks	Peridotites, felsic amphibolitic rocks	Continental rocks	Continental rocks
Protoliths of peridotites		Mantle wedge		Continental lithosphere		Mantle wedge	Mantle wedge & abyssal	Mantle wedge & abyssal		
P-T conditions	7 GPa 1100°C	2.7 GPa 850°C	3.4 GPa 675–775°C	3.2 GPa 840°C	2.0–2.6 GPa 870–930°C	3.2–3.3 GPa 764–820°C	4 GPa 700–800°C	>5.5 GPa 740–870°C	5.0 Gpa 560–600°C	6 Gpa 825–975°C
Metamorphic age	Cretaceous to Eocene	Early Paleozoic	Oligocene	Eocene	Miocene-Pliocene	Cambrian	Cambro-Ordovician	Triassic	Permian	Cambrian
Exhumation velocities	>8 mm/year	Unknown	>20 mm/year	Unknown	25 mm/year	>4 mm/year	6–8 mm/year	6 mm/year	Unknown	>18 mm/year
Exhumation timing	Microcontinent subduction	Collision	Syn-collision	Syn-collision	Back-arc spreading	Syn-subduction	Syn-collision	Syn-collision	Syn-collision	Syn-collision
Références	Liati, 2005	Nimis and Morten, 2000	Rubatto and Hermann, 2001	Nimis and Trommsdorf, 2001	Baldwin et al., 2004	Palmeri et al., 2007	Yang et al., 2003	Yang et al., 2003	Zhang et al., 2003	
	Perraki et al., 2006		Compagnoni and Rolfo, 2003		Monteleone et al., 2007		Hacker, 2006	Hacker, 2006		Hacker et al., 2003
								Liu et al., 2006		

Massif	Kaghan Pakistan	Tso Morari India	Sao Francisco Brazil	Gourma Mali	North Western gneiss region Norway	East Greenland	Bohemian massif Poland, Czech Republic	French Massif Central France	W. Gneiss Region Norway	Central Suwalesi
Abbreviation	KA	TSO	SAO	GOU	NWGR	EG	BO	FMC	WGR	CSU
Subduction context	Continental margin subduction	Continental margin subduction	Continental subdcution	Continental subdcution	Continental margin subduction	Continental margin subduction	Continental margin subduction	Continental margin subduction	Continental margin subduction	Oceanic subduction
Tectonics	3 nappes	3 nappes	2 nappes	3 nappes	2 nappes	1 nappe	5 nappes	3 nappes	2 nappes	>2 nappes
Lithology	Continental rocks	Upper continental rocks	Peridotites, felsic amphibolitic rocks	Continental rocks	Peridotites within gneisses	Continental rocks	Peridotites, felsic amphibolitic rocks	Peridotites, felsic amphibolitic rocks	Lower and upper continental rocks peridotites	Peridotites, serpentinites amphibolitic rocks
Protoliths of peridotites			Unknown		Mantle wedge		Mantle wedge & oceanic	Continental lithosphere		Oceanic
P-T conditions	3.0 GPa 720–820°C	3.9 Gpa 750–850°C	>2.8 GPA 750°C	>2.8 GPA 750°C	6.4–8 GPa 1200°C	3.6–4.2 GPa 928–972°C	up to 7.5 GPa up to 1335°C	3.0 GPa >750°C	3.5 GPa 700–800°C	>2.8 GPa 1100°C
Metamorphic age	Eocene	Paleocene	Pan-African	Pan-African	Silurian	Ordovician	Devonian	Devonian	Silurian	Cretaceous
Exhumation velocities	30–80 mm/year	17 mm/year	unknown	> > 4 mm/year	Unknown	Unknown	>6 mm/year	15 mm/year	8–12 mm/year	Unknow
Exhumation timing	Syn-collision	Syn-collision	Syn-collision	Syn-collision	Asthenospheric upwelling then syn-collision	Unknown	Syn-collision	Syn-collision	Syn-collision	Syn-subduction
Références	O'Brien et al., 2001 Treloar et al., 2003 Parrish et al., 2006	de Sigoyer et al., 2000 Guillot et al., 2003 Leech et al., 2005	Vaugh and Parkinson, 2003	Caby, 1994 Jahn et al., 2001	Van Roermund et al., 2001 Drury et al., 2001 Young et al., 2007	Gilotti and Krogh Ravna, 2002	Massonne, 2003 Medaris et al., 2004	Gardien et al., 1990 Lardeaux et al., 2001	Terry et al., 2000 Labrousse et al., 2002 Root et al., 2005	Parkinson et al., 1998

intrusions in shallow continental crust prior to the subduction as shown in Plate 3. The Caledonian UHP eclogites of Norway are considered to have originated from the lower crustal granulites of Precambrian age. However, the eclogitized granulites are associated with Precambrian gabbros, anorthosites and peridotites (Tucker et al., 1991). The occurrence of gabbro and peridotite with contemporanous gneiss suggests that these rocks were probably present in the continent-ocean transition where the lower crust is thin or totally absent. If this hypothesis is confirmed, it reinforces the idea that only the upper crust is exhumed.

Garnet peridotites have been described in UHP terranes in Phanerozoic continent-continent collision zones, including Dabie-Sulu terrane in China, Kokchetav massif in Kazakhstan, Western Gneiss Region in Norway, Alpe Arami in Switzerland and in the Palaeozoic belt of Europe (e.g., Medaris, 1999). They are classified into two types (e.g., Brueckner and Medaris, 2000; Zhang et al., 2000): (a) garnet peridotites originated from mantle wedges and tectonically incorporated within the subducting slab at great depth before its exhumation; (b) plagioclase-bearing cumulate ultramafic rocks emplaced at the base of the continental crust prior to the subduction and metamorphosed to garnet peridotites. In both cases, garnet peridotites are associated with continental rocks and their exhumation is explained by decoupling of the continental slice from the descending oceanic lithosphere due to the positive buoyancy of sialic continental rocks within the subduction channel (Van der Beuckel, 1992; Ernst, 1999, 2005).

The thickness of UHP domains varies widely. In the Western Alps, the Dora Maira UHP unit is 200 m in thickness and covers a surface area of about 25 km^2. In contrast, the Lower Paleozoic metamorphic domain in China forms an essentially continuous HP-UHP belt extending more than 4000 km from Quinlin to Dabie (Yang et al., 2003) with a thickness of 5 to 10 km (Hacker et al., 2000). Similarly, recent geochronological data confirm that the Western Gneiss Region in Norway forms a continuous HP-UHP unit of 200 × 400 × 5–10 km (Hacker, 2007; Young et al., 2007).

Primary magmatic texture in metamorphosed granite and volcanic rocks indicate locally low strain (Michard et al., 1993; de Sigoyer et al., 2004). High strain zones are found in most UHP units, such as the Dora Maira massif in the Alps (e.g., Michard et al., 1993), the Sulu and Dabie Shan massifs in China (e.g., Hacker et al., 2000; Zhao et al., 2005) and the Tso Morari and Kaghan units in Himalaya (e.g., Guillot et al., 2007). The evidence also indicates local high strain zone between these exhumed units from the dowgoing slabs. Based on the observation of the Himalayan UHP Tso Morari massif, Guillot et al. (2000) suggested, that the decoupling is controlled by the normal faults inherited from earlier rifts, making an upper crustal block easily dislodged from the rest of the subducting slab. This interpretation is analogous to that suggested by Jolivet et al. (2005) that the brittle to ductile transition of deformation plays an important role in decoupling the upper crust from the rest of the subducting lithosphere.

The progressive metamorphism of the Precambrian granulites in the Caledonian nappes of the Bergen Arc in Norway demonstrates the role of fluid circulation for eclogitization (Austrheim, 1994; Jolivet et al., 2005). Perhaps because of the presence of fluids, index minerals are poorly preserved in many UHP rocks of continental origin. This makes it difficult to define the boundary of an UHP domain. In fact, UHP rocks commonly record pressures ranging from about 2.5 GPa up to $P > 7$ GPa and temperatures varying between 500°C and 1335°C (Fig. 8). However, most UHP rocks of continental origin record pressures between 2.5 and 4.0 GPa (e.g., Hacker, 2006), and the UHP conditions are mostly recorded in garnet-bearing peridotites. The evidence suggests that mantle peridotites record an earlier event before their incorporation into the subduction channel due to an asthenospheric return flow (Fig. 8) (e.g., Spengler et al., 2006; Gorczyk et al., 2007).

UHP minerals are rarely preserved and mostly occur as relict in other minerals, such as coesite in garnet or omphacite or diamond in zircon. Nevertheless, their occurrence requires specific conditions, such as rapid cooling during decompression, rapid exhumation, fluid-absent condition during the exhumation and little deformation. These conditions are only locally attained so that the evidence for UHP conditions is only retained in lenses. UHP metamorphism records low geotherms ranging from 5 to 10°/km in most terranes, and down to 3.5°/km in the Forbidden Zone in China (Liou et al., 2000).

The P-T-t paths of UHP rocks are characterized by isothermal decompression until crustal depths (1.0 to 0.5 GPa). The absence of significant heat loss during the exhumation indicates their rapid exhumation, greater

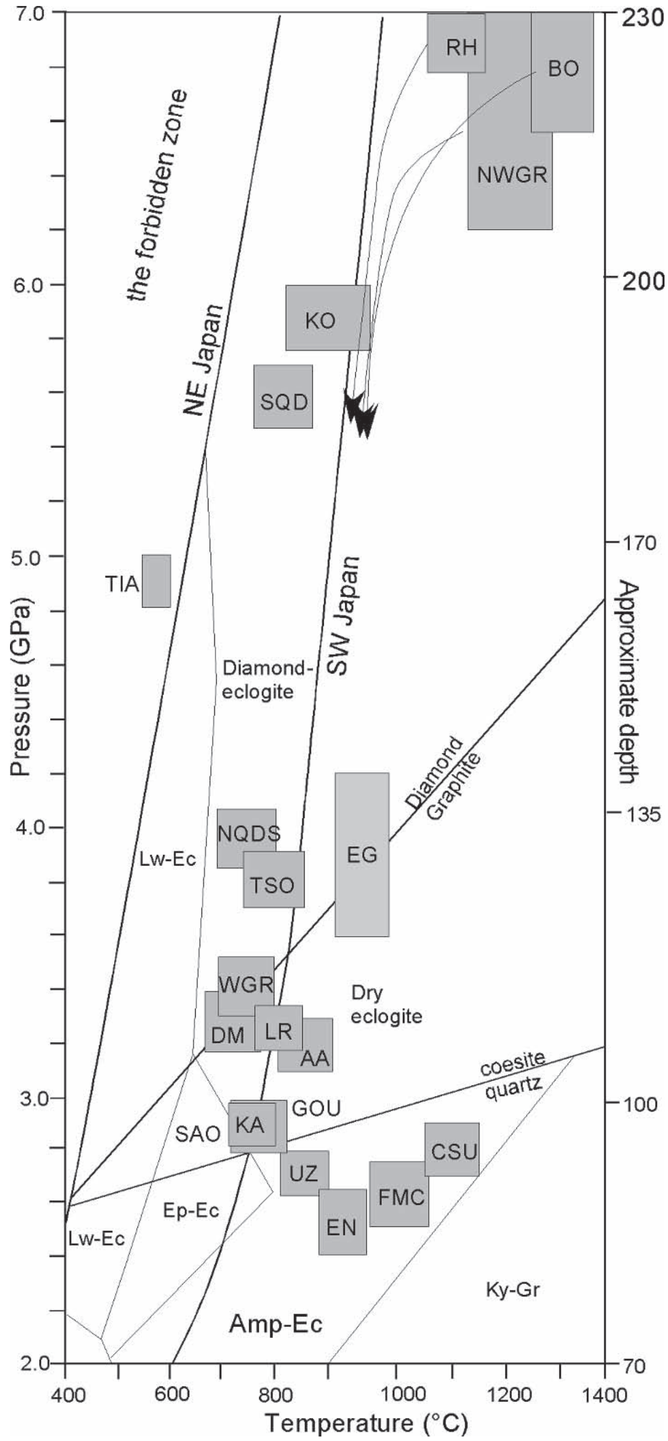

Fig. 8 Compiled P-T data for UHP rocks in continental and oceanic subduction complexes (see Table 3 for abbreviations of locations and references, and Fig. 5 for mineral abbreviations). The *arrows* show the asthenospheric upwelling of garnet peridotites before their integration in the subducting channels

than 3 mm/year (Duchêne et al., 1997; Grasemann et al., 1998). Estimated exhumation velocities in other UHP rocks of continental origin are also high, faster than 6 mm/year, reaching possibly up to 80 mm/year in the Alps and the Himalaya (Parrish et al., 2006) (Table 3). As for other types of subduction zones, the exhumation velocity is independent of the subduction velocity.

2 Discussion

2.1 Subduction Environments and the Timing of Exhumation

The common feature of the exhumation in the accretionary wedge environment and in the serpentinite-subduction channel environment is that both involve the subduction of oceanic lithosphere. The development of an accretionary wedge additionnally requires the offscraping of sediments derived from the lower plate or erosion of the upper plate. In the Western Alps, large proportions of these sediments (up to 50%) are exhumed, whereas only small fractions (<1%) of oceanic rocks are (Guillot et al., 2004; Agard et al., submitted). The metamorphosed oceanic rocks, blueschists-eclogites, are slowly exhumed (~ few mm/year) during active oceanic subduction. The peak pressures of those exhumed rocks are generally lower than 2.2 GPa, whereas peak pressures in serpentinite-subduction channel may reach the coesite stability field (2.8 Gpa, ZS; Fig. 7). The latter may contain garnet peridotites that were equilibrated at even higher pressures (~4 Gpa, RSJ; Fig. 7). Exhumation of sedimentary rocks lasts for a long time ranging from 25 Myr (Alpine Schistes Lustrés) to 100 Myr (Chile), whereas the exhumation of oceanic crust is commonly brief, less than 15–20 Myr (Agard et al., submitted). These authors have shown that the exhumation of oceanic lithosphere may occur shortly after the inception of subduction (Chile, Franciscan, Makran), in the midst of convergence (SE Zagros, NW Himalaya), or during the late stages of subduction (Western Alps, New Caledonia). Exhumed oceanic rocks are commonly associated with serpentinites. Exhumation velocities are also low, ranging between 1 and 5 mm/year. Exceptionally fast exhumation (~10 mm/year) in the western Alps is associated with later continental subduction (Agard et al., 2002; Guillot et al., 2004). The exhumation rates are independent of the subduction rates, confirming a decoupling between the subducting plate and the zone of exhumation.

Accretionary wedge and serpentinite subduction channel environments show two other major differences: the lithology and types of HP rocks. In accretionary wedge environment, HP rocks mostly originate from metasediments and form kilometric slices with continuous P-T conditions, frequently with higher pressure slices thrust over the lower pressure ones. On the other hand, serpentinite subduction channel is dominated by metabasites embedded in a sheared serpentinite matrix. These metabasite blocks record different P-T conditions, common in a tectonic mélange.

Note that an accretionary wedge and a serpentinite subduction channel may coexist in a single subduction zone at a given time, and exhumed rocks in these two settings may occur in close proximity in a subduction complex as shown in the Western Alps and the Franciscan (Fig. 9).

The continental-type subduction is accompanied by the exhumation of UHP rocks that were buried down to a depth between 100 and 200 km along cold geotherms. UHP rocks are exhumed rapidly (>6 mm/year) under isothermal conditions at the transition from oceanic subduction to continental collision. HP-UHP domains from 1 km to maximum 10 km thick nappe stacks over large surface areas (>50,000 km^2). Continuous UHP rocks of greater than 50 km in length are exposed in the Tso Morari area in the Himalaya, the Western Gneiss Region in Norway and Quinlin-Dabie in China. Due to its thickness and is positive buoyancy, the entire continental lithosphere cannot enter the subduction zone and stops within a couple of millions years after the initial contact of the continent with the trench. In the Himalaya, the thick buoyant upper Indian crust was blocked after 10 million years of continental subduction. It separated from the rest of the lithosphere and started to be stacked as nappes, which resulted in the high topographic relief in the area (Guillot et al., 2003). Similarly in the Caledonides, Hacker (2007) estimates that the UHP slab exhumed from mantle to crustal depth between 400 and 390 Ma.

As already discussed, accretionary wedge and serpentinite subduction channel can coexist in one subduction zone as observed in the Franciscan complex, the northern subduction complex in Dominican Republic, and the Western Alps. In other cases, serpentinite subduction channel may coexist with continental subduction, such as in Indonesia. The Alpine massif is

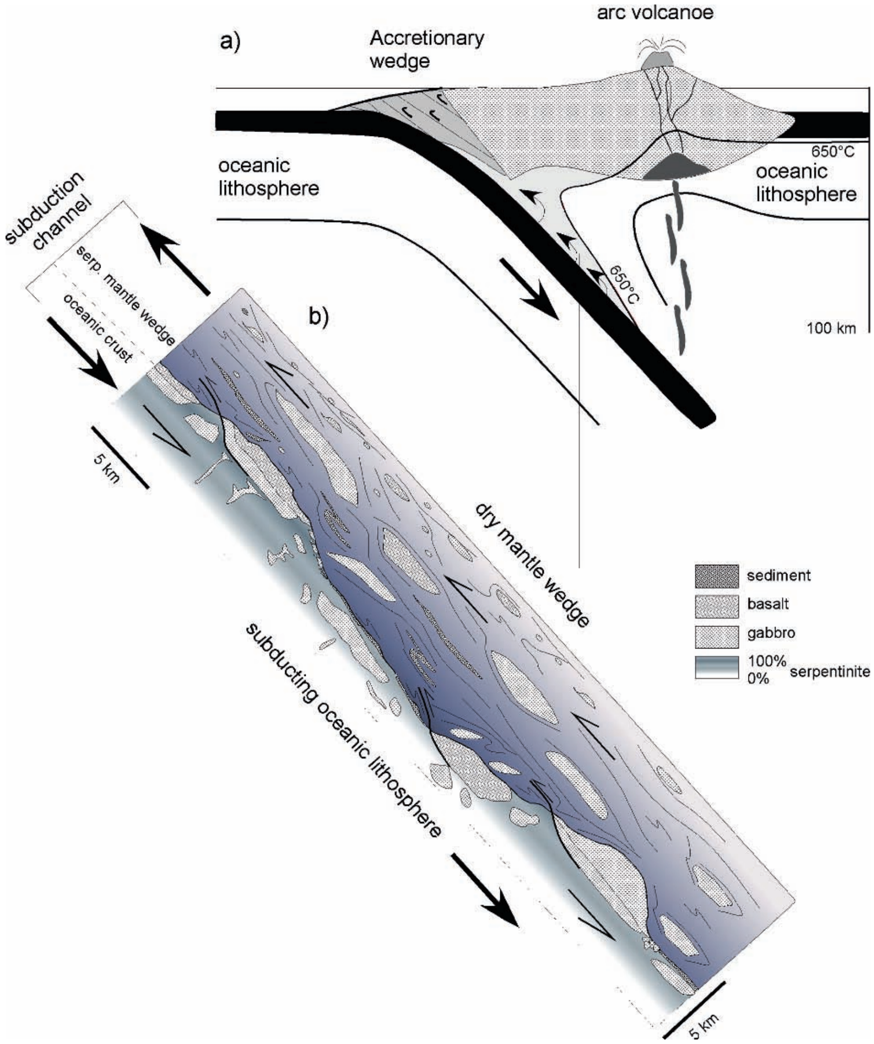

Fig. 9 (**a**) Schematic relationship between accretionary wedge and serpentinite subduction channel. The boundary between the serpentinite subduction channel is defined by the 650°C isotherm. (**b**) Detail of the serpentinite subduction channel. It forms a ~60 km long (from 40 to 100 km depth) soft channel between the dry (rigid) subducted oceanic lithosphere and the dry (rigid) mantle wedge. It is made of a melange of serpentinites deriving the hydrated oceanic lithosphere and from the hydration of the mantle wedge and contains exotic blocks of metabasalts, metasediments and metaggabros, mainly derived from the subducting oceanic lithosphere but also from the above arc system (e.g., Hattori and Guillot, 2007). Due to the low viscosity and low density of serpentinite mineral and the triangle shape of the serpentinite channel, the dowgoing material is progressively entrained upward (Guillot et al., 2001; Schwartz et al., 2001; Gerya et al., 2002)

probably the best exemple to depict the relationships between the three subduction types. Along a west-east traverse an accretionary wedge (the Schistes Lustés unit), a serpentinite channel (the Monviso unit) and a continental subduction unit (the Dora Maira unit) coexist. Several studies suggested that they correspond to the continuous evolution of a paleo-subduction zone from the Mid-Cretaceous to the Eocene (Agard et al., 2002; Schwartz et al., 2007; Yamato et al., 2007).

2.2 Essential Role of a Decoupling Zone

The opposite trajectories of exhumation and subduction require a decoupling zone within the subducting slabs. In fact, most of the subducted lithosphere is going down while only slices of their upper decoupled part make their way back to the surface, at certain time periods at the most (Agard et al., submitted). In oceanic subduction zones, the existence of a décollement layer is suggested at the ductile-britle transition. In accretionary wedge environment, the HP units form a nappe stack system thrusting in the direction of the paleo-trench with the lower grade metamorphic units at structurally lower levels (Fig. 4b). This observation is consistent with the off-scraping of the upper sedimentary layer in analogue models (Von Huene and Scholl, 1991; Glodny et al., 2005). In the case of serpentinite type subduction zones, several possible mechanisms contribute to the formation of the decoupling zone. Fluid migration in deep fractures is suggested to contribute to the formation of decoupling zones based on the occurrences of veins filled with eclogitic minerals (Philippot and Kienast, 1989). This field observation is compatible with geophysical data, suggesting dehydration-induced embrittlement of the subducting slab (Yamasaki and Seno, 2003). A serpentinized layer prior to subduction may become a decoupling zone between the oceanic crust and underlying lithospheric. This is compatible with the occurrence of boudinaged eclogitized metabasalts in serpentinites (e.g., Coleman, 1971; Philippot and Van Roermund, 1992; Blake et al., 1995; Schwartz et al., 2001; Vignaroli et al., 2005; Tsujimori et al., 2006).

In continental subduction zones, flat eclogitic ductile shear zones are documented, particularly in Norway (Jolivet et al., 2005). The shearing may exceeds the strength of the binding force of rocks and results in separating the buoyant upper crust from the denser lithosphere along a decollement. It is probable that quartzo-feldspathic upper crustal rocks at depths greater than 100 km are hot enough to be separated from the rest of sialic lithosphere (Stöckert and Renner, 1998). The proposed interpretation is significantly different from the model suggesting that the whole crust is decoupled from the subducting slab and exhumed by buoyancy forces (e.g., Chemenda et al., 1995). In contrast, our proposed model follows the concepts of Cloos (1982) and Platt (1986) suggesting the presence of a decoupling zone within the upper part of the subducting slab.

2.3 A Weak Subduction Channel Required for the Exhumation of HP to UHP Rocks

Fluids released from subducting slabs during progressive metamorphism facilitate the lubrication of the subduction plane but also assist the formation of low strength metamorphic minerals, such as lawsonite and phengite (Stöckert and Renner, 1998). In the case of accretionary-type subduction zones, these weak minerals can form high-strain shear zones, which localize the deformation and separates an exhumed block from the rest of the subducting slab. Moreover, lenses and blocks surrounded by shear zones remain relatively free from deformation and preserve HP mineral assemblages during exhumation. This concept is particularly pertinent to rigid metabasite blocks in a soft matrix of serpentinites in a serpentinite subduction channel (Fig. 10) (Blake et al., 1995; Schwartz et al., 2001; Gerya et al., 2002; Frederico et al., 2007). In the exhumation of continental rocks, the role of a weak zone has not been adequately addressed because buoyant continental rocks is considered to be sufficient for their exhumation of UHP rocks (e.g., Chemenda et al., 1995; Ernst, 2006), but the occurrence of serpentinites along the interface between the Tso Morari UHP unit and the overlying rigid mantle wedge (e.g., Guillot et al., 2001) suggest that a lubricating weak zone may be important in the exhumation of continental rocks.

The occurrence of garnet-bearing peridotites further supports the presence of a weak subduction channel. They are exhumed in an oceanic subduction zones in two locations: Higashi-Akaishi peridotite body in the Sanbagawa metamorphic belt in Japan and the Cuaba peridotites in the Rio San Juan complex in Dominican Republic. They are probably extreme cases where buoyant partly hydrated mantle facilitated the exhumation of deep rocks. Numerical models of Gorczyk et al. (2007) show that the steady state subduction does not result in the exhumation of garnet-bearing peridotites, but that hydration of deep mantle wedge modifies its rheology to allow the upwelling of the asthenospheric mantle wedge and subsequent retreat of the subducting slab. Slab retreat would induce exhumation of a deep-seated melange from a depth of 100–150 km that consists of UHP mafic rocks (subducted oceanic lithosphere), anhydrous peridotites, hydrated and partially molten peridotites of the mantle wedge.

2.4 Major Driving Forces for the Exhumation

It is easy to understand the cause of burial metamorphism, but the causes of exhumation are less easily understood. Exhumation of HP to UHP metamorphic

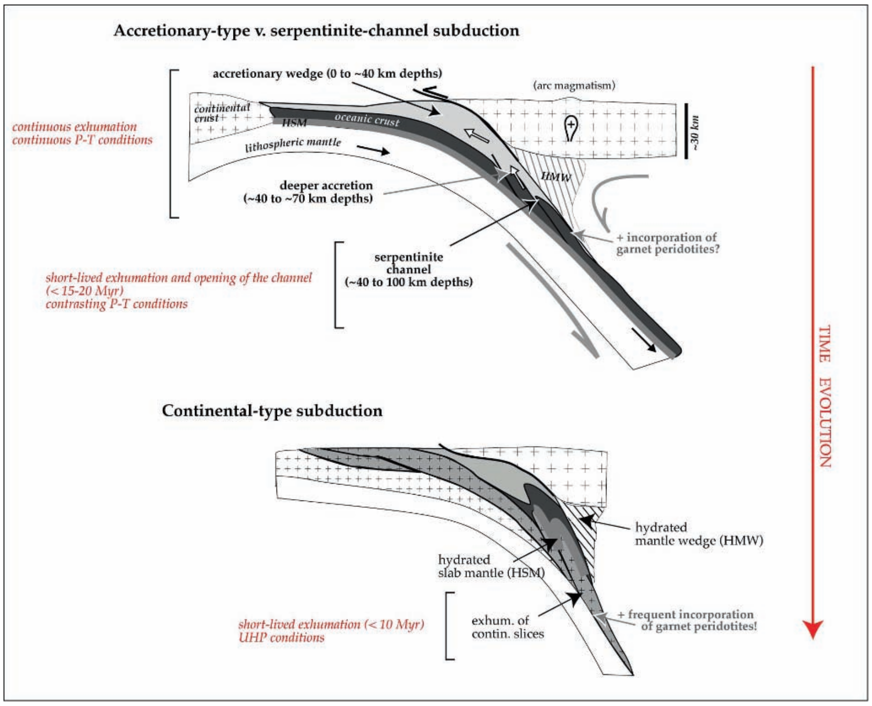

Fig. 10 Schematic model for the exhumation of HP-UHP rocks inferred from the tectonic evolution of the Piedmont zone (Western Alps) during Late-Cretaceous-Paleogene. During the oceanic subduction period: developped an accretionary wedge and a serpentinite channel. During short-lived period, HP rocks and locally UHP rocks (garnet bearing peridotites) exhumed. The implication of the continental lithosphere within the subduction increase the buoyancy, allowing the final exhumation of the accretionary wedge and the serpentinite channel. Slices of upper continental rocks incorporate mantle peridotites and exhumed rapidly within the suture zone

rocks requires a combination of several factors; buoyancy of rocks, a mechanism to reduce the boundary forces between these rocks, the descending lithosphere (Jolivet et al., 2005), erosion of overlying rocks, thrusting associated with normal faulting, and return flow inside the subduction channel. Metamorphism and fluids play an important role in changing the density of rocks, the balance of forces (Hacker, 1996; Le Pichon et al., 1997) and softening of eclogitized rocks (Hacker, 1996; Jolivet et al., 2005).

In the following paragraphs we will discuss these physical parameters for the exhumation of HP to UHP rocks in oceanic or continental context.

In a subduction zone, two types of forces contribute to the exhumation of HP to UHP rocks: the boundary forces related to the subduction zone itself and the internal forces induced by the density difference between the subducting slab and the surrounding rocks. The eclogitization of oceanic crust makes it denser than the surrounding mantle peridotites, and further promotes the subduction process. This implies that the exhumation of metamorphosed oceanic crust requires other factors than buoyancy. In accretionary wedges, metasediments with low densities (ca. 3,000 kg/m^3) are not easily subducted with dense metabasic rocks (>3,200 kg/m^3), which leads to their decoupling from the subducting salb and underplating at the base of the accretionary wedge. Platt (1986, 1987) proposed that this underplating process coupled with shallow extension would allow HP rocks to be exhumed to upper crustal levels. We argue against this proposal. First, most modern sedimentary accretionary wedges are not deep enough to produce HP rocks. The formation of these HP rocks requires unusually deep accretionary prisms. Secondly, exhumation frequently occurs during a short period in a given subduction zone (~15 Myr; Agard et al., 2006; Agard et al., submitted), suggesting that such a steady-state regime suggested by Platt would not lead to the exhumation of HP rocks. Fig. 3d shows the schematic section of the present-day

Cascadia accretionary wedge beneath the Vancouver Island (Fig. 2a), but it must be noted that no exhumation is happening at present within the active Cascadia accretionary wedge. This confirms that the exhumation of HP rocks likely takes place during the perturbation of subduction zones as suggested by Agard et al. (2006) and others. The perturbations include a change in subduction velocity or subduction angle, and docking of a seamount, an arc or a continental block.

Within a serpentinite subduction channel, the exhumation of dense mafic rocks is facilitated by low density (2,600 kg/m^3) and low viscosity of serpentine minerals. Low density of serpentinites results in diapiric ascent of serpentinites in the Mariana forearc (Fryer et al., 1999). Buoyancy of serpentinites likely contributed to the exhumation of Monviso massif in the Alps. The average density of the entire Monviso massif including eclogites is about 2,850 kg/m^3, which is lower than anhydrous mantle peridotites. Moreover, the low viscosity of serpentinite induces a dynamic flow inside the subduction channel (Schwartz et al., 2001; Gerya et al., 2002; Hilairet et al., 2007). A return flow within the serpentinite subduction channel can exhume dense eclogitic blocks (Cloos, 1982). This return flow is enhanced by the progressive dehydration of serpentinites at the depth where the subducting slab reaches the temperature of 650–700°C (Fig. 11). The temperature of 650–700°C is reached at a depth of about 100 km, ~2.8 GPa, which coincides with the maximum pressures recorded in eclogites in serpentinite melanges (Fig. 7).

In the continental-type subduction environment, the upper crust is firmly attached to the sinking lithosphere. Furthermore, sialic crustal rocks remain buoyant during subduction because their density is not significantly modified during subduction. Main hydrous phases, phengite and mica, are stable even during UHP metamorphism. Decoupling of a crustal slice from the descending slab requires the buoyancy forces exceeding the strength of the upper crust, which may occur at a depth of 90 to 140 km (Fig. 12b). Buoyancy difference between the continental rocks and oceanic lithosphere likely results in the separation of the two by thrusting along the subduction plane and normal faulting at shallower depth (Figs. 12a, b). Finally, the detachment of oceanic lithosphere further enhances the buoyant exhumation of the continental crust and sinking of the oceanic lithosphere (Fig. 12d) (Van der Beuckel, 1992; Davies and von Blanckenburg, 1995). However, this last model implies large uplift during exhumation incompatible with exhumation occurring beneath sea level as observed for exemple in Himalaya (e.g., Guillot et al., 2003) or in the Alps (e.g., Tricart et al., 2004).

2.5 Other Factors Contributing to Exhumation

Several other factors contribute to the exhumation of HP to UHP rocks. Slab retreat has been invoked as an important cause for the exhumation of HP rocks in the Mediterranean domain as it creates an extensional regime for the exhumation (e.g., Gautier et al., 1999; Jolivet et al., 2003). As previously discussed, slab retreat and associated back-arc extension are suggested to explain the exhumation of deep seated garnet-peridotites in the Dominican Republic (Gorczyk et al., 2007) and also the world youngest eclogite in Papua New Guinea (Monteleone et al., 2007). In the numerical model developed by Gorczyk et al. (2007), the role of asthenospheric upwelling is essential in rapid exhumation of deep-seated garnet-bearing peridotites. Similarly, the occurrence of majoritic garnet in the Western Gneiss Region of Norway (Van Roermund et al., 2001) and the recent discovery of coesite possibly replacing stishovite in non-metamorphic chromitite in southern Tibet (Yang et al., 2007) suggest that rocks originated from the deep upper mantle (>300 Km) are exhumed within suture zones. Exhumation of such deep rocks near the the mantle transition zone suggest a large-scale convection in the upper mantle.

Subduction angle is also important in controlling the production and exhumation of HP and UHP rocks. Guillot et al. (2007) estimated that the initial angle of continental subduction was greater than 40° in the western Himalayan syntaxis. Such a steep subduction is displayed in tomographic images to a depth of 200–300 km beneath the Hindu Kush and supported by seismic studies (Negredo et al., 2007). The evidence suggests that the UHP metamorphic rocks are being formed in the slab beneath the Hindu Kush at present (Searle et al., 2001). In contrast, tomographic images and seismic data show that the Indian continent subducted at a gentle angle of 9° beneath southern Tibet, reaching a depth of less than 80 km (<2.0–2.5 GPa), which precludes the formation of UHP rocks in the area (Guillot et al., 2008).

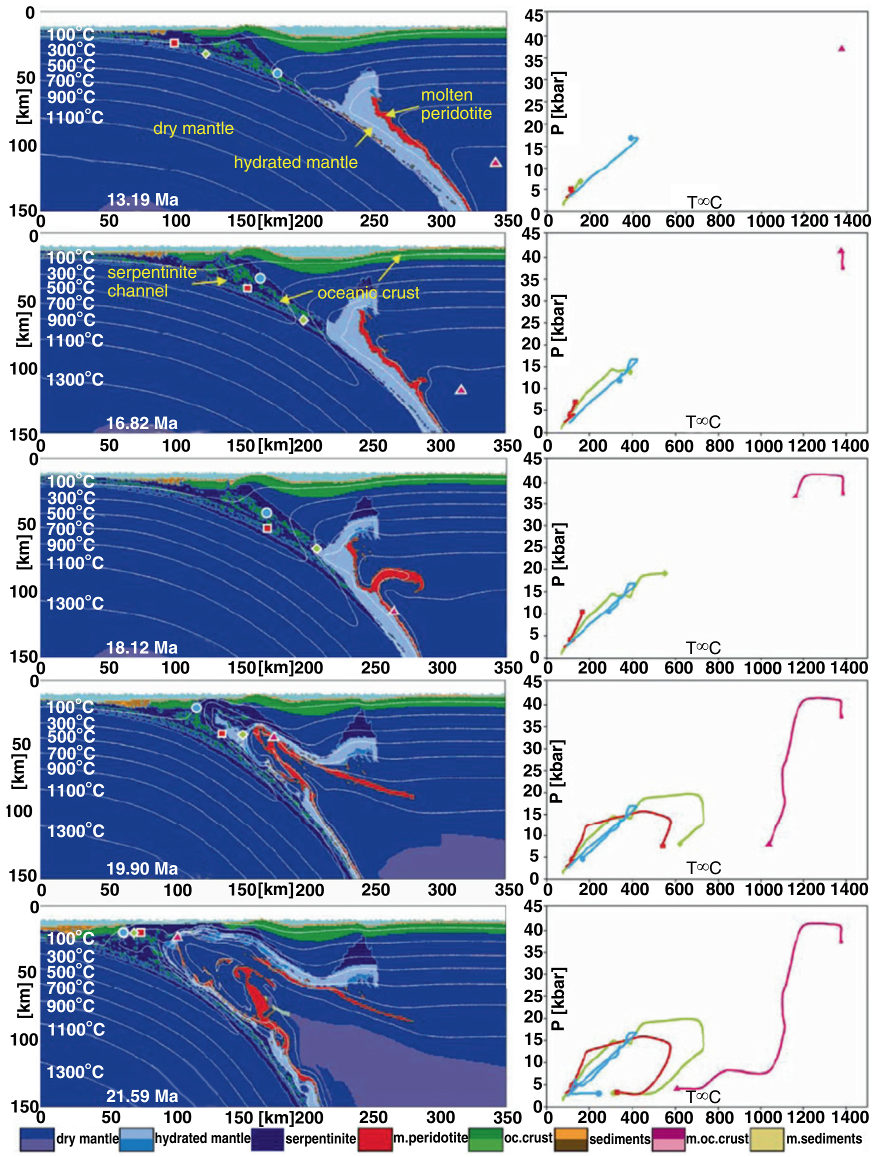

Fig. 11 Evolution of a subduction of oceanic lithosphere that formed at slow spreading ridge (after Gorczyk et al., 2007). The numerical model shows that the subduction produces a wide subduction channel composed of serpentinites because oceanic lithosphere formed at a slow-spreading ridge contain abundant serpentinites. The numerical model predicts two kinds of serpentinites within the subduction channel: (a) incoming hydrated abyssal peridotites and (b) hydrated, forearc mantle peridotites. The maximum depth of circulating material in the serpentinite subduction channel reaches a depth of 60 km (~2 GPa) and a temperature of 740°C, which corresponds to the upper stability limit of serpentine minerals (Ulmer and Trommsdorff, 1995). Progressive hydration of the mantle wedge modifies its rheology allowing the upwelling of the asthenospheric mantle wedge and subsequent retreat of the subducting slab. Slab retreat would induce exhumation of deep-seated melange from a depth of 100–150 km that consists of UHP mafic rocks (subducted oceanic lithosphere), anhydrous peridotites, hydrated and partially molten peridotites of the mantle wedge. This deep-seated melange would not reach the surface and stops at about 20 km depth beneath the already exhumed serpentinite melange

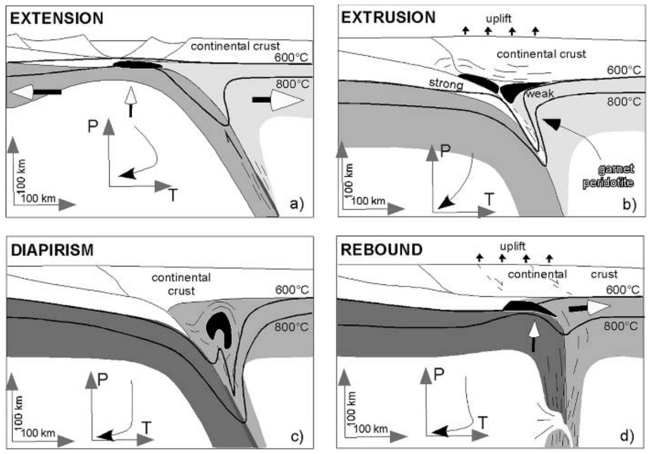

Fig. 12 Summary of UHP models (modified after Young et al., 2007). (**a**) Exhumation of subducted oceanic rocks by local extension. This model cannot exhume rocks from a depth greater than 100 km because a horizontal extension of greater than 200 km at crustal level is requires. Extrusion of delaminated dowgoing slab due to buoyancy forces with thrusting at the base and normal faulting at the top (Ernst, 2001, 2005). This model explains incorporation of deep mantle garnet peridotites. (**b**) Diapiric ascent of delaminated UHP rocks combined with horizontal compression in overlying plate (e.g., de Sigoyer et al., 2004). (**c**) Separation of continental rocks from descending oceanic lithosphere followed by flexural rebound of the UHP unit (Young et al., 2007)

The important role of steep subduction in the formation and subsequent exhumation of UHP rocks is further illustrated in the Alpine and Himalayan systems. The subducted European continental margin shows up to 1.2 GPa and 450°C in the central part and up to 3.5 GPa and 750°C in the southern part, suggesting that the dip steepened from 40° to 70° southward (e.g., Carry, 2007). As for the Himalayan system, the dips of subducting plate change along a transform fault and the exhumation of UHP rocks occur near the transform fault.

3 Conclusions

The P-T-t paths and protoliths of HP and UHP metamorphic rocks provide information relevant to a better understanding of subduction zones. The combination of data from metamorphic rocks with numerical models draws the following salient results:

– The exhumation of HP to UHP rocks including those originated from continental rocks is an integral part of subduction processes.
– Exhumation of rocks requires mechanically weak subduction channels that are comprised of sediments, hydrated peridotites or partial melt.
– The driving forces for exhumation are a combination of buoyancy and channel flow coupled with underplating of slabs. The former is the dominant force for the exhumation of continental rocks, whereas the latter prevails for the exhumation in oceanic subduction zones.
– Exhumation velocities are independent of plate velocities: (1) slow (<5 mm/year) exhumation of HP-LT metasediments ($P < 2.5$ GPa, $T < 600$°C) is a long-lasting process, in an accretionary prism; (2) slow to intermediate velocity ($1 < v < 10$ mm/year) exhumation of HP to UHP (< 3 GPa < 650°C) oceanic rocks is a discontinuous, transient process within a serpentinite subduction channel; (3) fast exhumation (up to 40 mm/year) of UHP (up to 6 GPa, 900°C) continental units is extremely short-lived (<10 My) and occurs in the mantle wedge combined with both asthenospheric return flow and buoyancy forces.
– Other parameters that affect the exhumation of HP to UHP rocks include slab retreat, and subduction dip angle. UHP rocks are not produced in subduction zones with gentle subduction angles.

Acknowledgments We thank W.G. Ernst and F. Rossetti for their helpful suggestions, which improved the quality of the manuscript. The work was supported by grants from "Dyeti" CNRS program and NSERC of Canada.

References

Abbott RN, Draper G and Broman BN (2006) P-T path for ultra-high-pressure garnet ultramafic rocks of the Cuaba gneiss, Rio San Juan complex, Dominican Republic. Int Geol Rev 28: 778–790.

Agard P, Monié P, Jolivet L and Goffé B (2002) Exhumation of the Schistes Lustrés complex: in situ laser probe Ar/Ar constraints and implications for the Western Alps. J Metam Geol 20: 599–618.

Agard P, Labrousse L, Elvevold S and Lepvrier C (2005) Discovery of Paleozoic Fe-Mg carpholite in Motalfjella, Svalbard Caledonides: a milestone for subduction-zone gradients. Geology 33: 761–764.

Agard P, Monié P, Gerber W, Omrani J, Molinaro M, Meyer B, Labrousse L, Vrielynck B, Jolivet L and Yamato P (2006) Transient, synobduction exhumation of Zagros blueschits inferred from P-T, deformation, time and kinematic constraints: implications for Neotethyan wedge dynamics. J Geophys Res 111 doi:10.1029/2005JB004103.

Agard P, Yamamoto P, Jolivet L and Burov E (2008) Discontinuous exhumation of oceanic crust: insights from blueschists and eclogites into the subduction channel: Earth Science Reviews, in press.

Aitchinson JC, Blake C, Flood PG and Jayko AS (1994) Paleozoic ophiolitic assemblages within the southern New England Orogen of eastern Australia: implications for growth of the Gondwana margin. Tectonics 13: 1135–1149.

Allemand P and Lardeaux JM (1997) Strain partioning and metamorphism in a deformable orogenic wedge: application to the Alpine belt. Tectonophysics 280: 157–169.

Altherr R, Marschall H and Ludwig T (2004). Evolution of a tourmaline-bearing lawsonite eclogite from the Elekdag area (Central Pontides, N Turkey): evidence for infiltration of slab-derived B-rich fluids during exhumation. Contrib Mineral Petrol 148: 409–425.

Anczkiewicz R, Burg JP, Villa IM and Meier M (2000) Late Cretaceous blueschist metamorphism in the Indus suture zone, Shangla region, Pakistan Himalaya. Tectonophysics 324: 111–134.

Anczkiewicz R, Platt JP, MF T and Wakabayashi J (2004) Franciscan subduction off to a slow start: evidence from high-precision Lu–Hf garnet ages on high grade-blocks. Earth Planet Sci Lett 225: 147–161.

Arculus RJ, Lapierre H and Jaillard E (1999) Geochemical window into subduction and accretion processes; Raspas metamorphic complex, Ecuador. Geology 27: 547–550.

Augier R, Agard P, Monié P, Jolivet L, Robin C and Booth-Rea G (2005) Exhumation, doming and slab retreat in the Betic Cordillera (SE Spain): in-situ $^{40}Ar/^{39}Ar$ ages and P-T-d-t paths for the Nevado-Filabride complex. J Metam Geol 23: 357–381.

Austrheim H (1994) Eclogitization of the deep crust in continent collision zones. C R Acad Sci 319: 761–774.

Auzende AL, Guillot S, Devouard B and Baronnet A (2006) Serpentinites in Alpine convergent setting: effects of metamorphic grade and deformation on microstructures. Eur J Mineral 18: 21–33.

Avé Lallemant HG and Sisson VB (2005) Exhumation of eclogites and blueschists in northern Venezuela: Constraints from kinematic analysis of deformation structures: in Avé Lallemant HG and Sisson VB eds., Caribbean/South American plate interactions, Venezuela: Geological Society of America Special Paper 394: 193-206.

Baldwin SL, Monteleone B, Webb LE, Fitzerald PG, Grove M and Hill EJ (2004) Pliocene eclogite exhumation at plate tectonic rates in eastern Papua New Guinea. Nature 431: 263–267.

Bally AW (1981) Thoughts on the tectonics of folded belts. In: Price NJ and McClay (eds) Thrust and Nappe Tectonics. Spec Pub Geol Soc London 9: 13–32.

Beaumont C, Ellis D and Pfiffner A (1999) Dynamics of sediment subduction-accretion at convergent margins: short-term modes, long-term deformation, and tectonic implications. J Geophys Res 104: 573–602.

Blake C, Moore DG and Jayko AS (1995) The role of the serpentinite melange in the unroofing of the UHP rocks: an example from the western Alps in Italy. In: from Coleman RG and Wang X (eds) Ultrahigh pressure metamorphism Cambridge University Press: 182–205.

Bosse V, Féraud G, Ballèvre M, Peucat JJ and Corsini M (2005) Rb-Sr and Ar-Ar ages in blueschists from the Ile de Groix (Armorican Massif, France): implications for closure mechanisms in isotopic systems. Chem Geol 220: 21–45.

Bostock MG, Hyndman RD, Rondenay S and Peacock SM (2002) An inverted continental Moho and serpentinization of the forearc mantle. Nature 417: 536–538.

Brueckner HK and Medaris LG (2000) A general model for the intrusion and evolution of 'mantle' garnet peridotites in high-pressure and ultrahigh pressure metamorphic terranes. J Metam Geol 18: 123–133.

Caby R (1994) Precambrian coesite from northern Mali: first record and implications for plate tectonics in the Trans-Saharan segment of the Pan-African belt. Eur J Mineral 6: 235–244.

Caby R, Buscail F, Dembélé D, Diakité S, Sacko S and Bal M (2008) Neoproterozoic garnet-glaucophanites and eclogites: new insights for subduction metamorphism of the Gourma fold- and- thrust belt (eastern Mali): Geological Society of London Special Publication 297: 203-216.

Caron JM and Péquignot G (1986) The transition between blueschists and lawsonite-bearing eclogites based on observations from Corsican metabasites. Lithos 19: 205–218.

Carswell DA (1990) Eclogite facies rocks. Blackie, Glasgow and London: 396p.

Carry N (2007) De la subduction continentale à l?exhumation dans les Alpes Penniques – Modélisation thermo-mécanique et paléogéographique.: Ph-D University of Rennes, 311 p.

Chemenda AI, Mattauer M, Malavieille J and Bokun AN (1995) A mechanism for syn-collisional rock exhumation and associated normal faulting: results from physical modelling. Earth Planet Sci Lett 132: 225–232.

Chopin C (1984) Coesite and pure pyrope in high-grade blueschists of the Western Alps. Contrib Minreal Petrol 86: 107–118.

Cloos M (1982) Flow melanges: numerical modelling and geological constraints on their origin in the Franciscan subduction complex. Geol Soc Am Bull 93: 330–345.

Cloos M and Shreve RL (1988) Subduction channel model of prism accretion, melange formation, sediment subduction, and subducting erosion at convergent plate margins: 1.

Background and description, in subduction zone Part 1. Pageophysics 128: 501–545.
Cluzel D, Aitchinson JC and Picard C (2001) Tectonic accretion and underplating of mafic terranes in the Late Eocene intraoceanic fore-arc of New Caledonia (Southwest Pacific): geodynamic implications. Tectonophysics 340: 23–60.
Coleman RG (1971) Plate tectonic emplacement of upper mantle peridotites along continental edges. J Geophys Res 76: 1212–1222.
Collins AS, Reddy S, Buchan C and Mruma A (2004) Temporal constraints on Paleoproterozic eclogite formation and exhumation (Usagaran Orogen, Tanzania). Earth Planet Sci Lett 224: 175–192.
Compagnoni R and Maffeo B (1973) Jadeite-bearing metagranite l.s. and related rocks in the Monte Mucrone area (Sesia Lanzo zone, Western Italian Alps). Schweiz Mineral Petrog Mitt 53: 355–377.
Compagnoni R and Rolfo F (2003) UHPM units in the western Alps. EMU notes in Mineralogy 5: 13–49.
Davies J and von Blanckenburg F (1995) Slab breakoff: a model of lithosphere detachement and its test in the magmatism and deformation of collisional orogens. Earth Planet Sci Lett 129: 85–102.
de Sigoyer J, Chavagnac V, Blichert-Toft J, Villa IM, Luais B, Guillot S, Cosca M and Mascle G (2000) Dating the Indian continental subduction and collisional thickening in the northwest Himalaya: multichronology of the Tso Morari eclogites. Geology 28: 487–490.
de Sigoyer J, Guillot S and Dick P (2004) Exhumation Processes of the high-pressure low-temperature Tso Morari dome in a convergent context (eastern-Ladakh, NW-Himalaya). Tectonics 23: TC3003 – 10.1029/2002TC001492.
Dewey JF, Ryan PD and Andersen TB (1993) Orogenic uplift and collapse, crustal thickness, fabrics and metamorphic phases changes: the role of eclogites Geol Soc Spe Pub. In: Prochard HM, Alabaster T, Harris NBW and Neary CR (eds) Magmatic Processes and Plate tectonics, 325–343.
Dobretsov NL and Buslov MM (2004) Serpentinite mélanges associated with HP and UHP rocks in central Asia. Int Geol Rev 46: 957–980.
Drury MR, Van Roermund HLM, Carswell DA, De Smet JH, Van der Berg AP and Vlaar NJ (2001) Emplacement of Deep Upper-mantle rocks into cratonic lithophere by convection and diapiric upwelling. J Petrol 42: 131–140.
Duchêne S, Lardeaux JM and Albarède F (1997) Exhumation of eclogites: insights from depth-time path analysis. Tectonophysics 280: 125–140.
Enami M, Mizukami T and Yokoyam K (2004) Metamorphic evolution of garnet-bearing ultramafic rocks from the Gongen area, Sanbagwa belt, Japan. J Metam Geol 22: 1–15.
Erdmer P, Ghent E, Archibald D and Stout M (1998) Paleozoic and Mesozoic high-pressure metamorphism at the margin of ancestral North America in central Yukon. Geol Soc Am Bull 110: 615–629.
Ernst WG (1973) Blueschist metamorphism and P-T regimes in active subduction zones. Tectonophysics 17: 255–272.
Ernst WG (1999) Metamorphism, partial preservation, and exhumation of ultrahigh-pressure belts. Isl Arcs 8: 125–153.
Ernst WG (2001) Subduction, ultrahigh-pressure metamorphism, and regurgitation of buoyant crustal slices – implications for arcs and continental growth. Phys Earth Planet Inter 127: 253–275.
Ernst WG (2005) Alpine and Pacific styles of Phanerozic mountain building: subduction-zone petrogenesis of continental crust. Terra Nova 17: 165–188.
Ernst WG (2006) Preservation/exhumation of ultrahigh-pressure subduction complexes. Lithos 92: 321–335.
Escuder-Viruete J and Pérez-Estaùn A (2006) Subduction-related P-T path for eclogites and garnet glaucophanites from the Samanà Peninsula basement complex, northern Hispaniola. Int J Earth Sci 95: 995–1017.
Fitzherbert JA, Clarke GL and Powell R (2005) Preferential retrogression of high-*P* metasediments and the preservation of blueschist to eclogite facies metabasite during exhumation, Diahot terrane, NE New Caledonia. Lithos 83: 67–96.
Forster MA and Lister G (2005) Several distinct tectono-metamorphic slices in the Cycladic eclogite-blueschist belt, Greece. Contrib Mineral Petrol 150: 523–545.
Fotoohi Rad GR, Droop GTR, Amini S and Moazzen M (2005) Eclogites and blueschists of the Sistan Suture Zone, eastern Iran: a comparison of P–T histories from a subduction mélange. Lithos 84: 1–24.
Frederico L, Crispini L, Scambelluri M and Capponi G (2007) Ophiolite mélange zone records exhumation in a fossil subduction channel. Geology 35: 499–502.
Fryer P, Wheat CG and Mottl MJ (1999) Mariana blueschist mud volcanism: implications for conditions within the subduction zone. Geology 13: 103–106.
Furukawa Y (1993) Depth of the decoupling plate interface and thermal structure under arcs. J Geophys Res 98: 20005–20013.
Gabriele P, Ballèvre M, Jaillard E and Hernandez J (2003) Garnet-chloritoid-kyanite metapelites from the Raspas Complex (SW Ecuador): a key a key eclogite-facies assemblage. Eur J Mineral 15: 977–989.
Garcia-Casco AG, Torres-Roldan RL, Millan Trujillo G, Monié P and Schneider J (2002) Oscillatory zoning in eclogitic garnet and amphibole northern serpentinite melange, Cuba: a record of tectonic instability. J Metam Geol 20: 581–598.
Gardien V, Tegyey M, Lardeaux JM, Misseri M and Dufour E (1990) Crust-mantle relationships in the French Variscan chain: the example of the southern Monts du Lyonnais (MCF). J Metam Geol 8: 477–492.
Gautier P, Brun JP, Moriceau R, Sokoutis D, Martinod J and Jolivet L (1999) Timing, kinematics and cause of Aegean extension: a scenario based on a comparison with simple analogue experiments. Tectonophysics 315: 31–72.
Gerya TV, Stöckert B and Perchuck AL (2002) Exhumation of high pressure metamorphic minerals in subduction channels: a numerical simulations. Tectonics 21: 1056, doi:10.1029/2002TC001406.
Ghent E, Stout M and Erdmer P (1993) Pressure–temperature evolution of lawsonite-bearing eclogites, Pinchi Lake, British Columbia. J Metam Geol 11: 279–290.
Gilotti JA and Krogh Ravna EJ (2002) First evidence for ultrahigh-pressure metamorphism in the north- east Greenland Caledonides. Geology 30: 551–554.
Glodny J, Lohrmann J, Echtler H, Gräfe K, Seifert W, Collao S and Figueroa O (2005) Internal dynamics of a paleoaccretionary wedge: insights from combined isotope tectonochronology and sandbox modelling of the South-Central Chilean forearc. Earth Planet Sci Lett 231: 23–39.

Godard G (2001) Eclogites and their geodynamic interpretation: a history. J Geodyn 32: 165–203.

Goncalvez P, Guillot S, Nicollet C and Lardeaux JM (2000) Thrusting and sinistral wrenching in a pre-Eocene carribean accretionary wedge (Samana pensinsula -Dominican Republic). Geodin Acta 13: 119–132.

Gorczyk W, Guillot S, Gerya TV and Hattori K (2007) Asthenospheric upwelling, oceanic slab retreat and exhumation of UHP mantle rocks: insights from Greater Antilles. Geophys Res Lett 34: L211309, doi:10.1029/2007GL031059.

Grasemann B, Ratsbacher L and Hacker BR (1998) Exhumation of ultrahigh-presssure rocks: thermal boundary conditions and cooling history. In "When continent collide: Geodynamics and Geochemistry of Ultrahigh-pressure rocks" edited by BR Hacker and JG Liou, Springer New York, 21:117–139.

Guillot S, Hattori K and Sigoyer de J (2000) Mantle wedge serpentinization and exhumation of eclogites: insights from eastern Ladakh, northwest Himalaya. Geology 28: 199–202.

Guillot S, Hattori K, Sigoyer de J, Nägler T and Auzende AL (2001) Evidence of hydration of the mantle wedge and its role in the exhumation of eclogites. Earth Planet Sci Lett 193: 115–127.

Guillot S, Garzanti E, Baratoux D, Marquer D, Mahéo G and de Sigoyer J (2003) Reconstructing the total shortening history of the NW Himalaya. Geochem Geophys Geosyst 4(1) doi:10.1029/2002GC000484.

Guillot S, Schwartz S, Hattori K, Auzende A and Lardeaux JM (2004) The Monviso ophiolitic Massif (Western Alps), a section through a serpentinite subduction channel. In: Beltrando M, Lister G, Ganne J and Boullier A (eds) Evolution of the western Alps: insights from metamorphism, structural geology, tectonics and geochronology. J Virtual Explorer 16: Paper 6.

Guillot S, Replumaz A, Hattori K and Strzerzynski P (2007) Initial Geometry of Western Himalaya and Ultra-High Pressure Metamorphic Evolution. J Asian Earth Sci 30: 557–564.

Guillot S, Mahéo G, de Sigoyer J, Hattori KH and Pêcher A (2008) Tethyan and Indian subduction viewed from the Himalayan high- to ultrahigh-pressure metamorphic rocks. Tectonophyics doi:10.1016/j.tecto.2007.11.059.

Hacker BR (1996) Eclogite formation and the rheology, buoyancy, seismicity, and H2O content of oceanic crust. In: Bebout GE, Scholl DW, Kirby SH and Platt JP (eds) Geophysical Monograph Series, Subduction top to Bottom, 96: 337–346.

Hacker BR (2006) Pressure and Temperature of Ultrahigh-Pressure metamorphism: implications for UHP Tectonics and H20 in Subducting slabs. Int Geol Rev 48: 1053–1066.

Hacker BR (2007) Ascent of the ultrahigh-pressure Western Gneiss Region, Norway. In: Cloos M, Carlson WD, Gilbert MC, Liou JG and Sorensen SS (eds) Convergent Margin Terranes and Associated Regions: A tribute to WG Ernst: Geological Society of America Special Paper 419: doi: 101130/2006.211909.

Hacker BR, Ratschbacher L, Webb L, MCWilliams MO, Ireland T, Calvert A, Dong S, Wenk, HR and Chateigner D (2000) Exhumation of ultrahigh-pressure continental crust in east central China: Late Jurassic-Early Jurassic tectonic unroofing. J Geophys Res 105: 13339–13364.

Hacker BR, Calvert A, Zhang RY, Ernst WG and Liou JG (2003) Ultrarapid exhumation of ultrahigh-pressure diamond-bearing metasedimentary rocks of the Kokchetav Massif, Kazakhstan. Lithos 70: 61–75.

Harlow GE, Hemming SR, Avé Lallemant HG, Sisson VB and Sorensen SS (2004) Two high-pressure-low-temperature serpentinite-matrix mélange belts, Motagua fault zone, Guatemala: a record of Aptian and Maastrichian collisions. Geology 32: 17–20.

Hattori KH and Guillot S (2007) Geochemical character of serpentinites associated with high- to ultrahigh-pressure metamorphic rocks in the Alps, Cuba, and the Himalayas: recycling of elements in subduction zones. Geochem Geophys Geosyst 8: Q09010, doi:10.1029/2007GC001594.

Haüy RJ (1822) Traité de Minéralogie. Seconde édition, Bachelier et Huzard, Paris.

Hermann J, Müntener O and Scambelluri M (2000) The importance of serpentinite mylonites for subduction and exhumation of oceanic crust. Tectonophysics 327: 225–238.

Hilairet N, Reynard B, Wang Y, Daniel I, Merkel S, Nishiyama N and Petitgirard S (2007) High-Pressure Creep of Serpentine, Interseismic Deformation, and Initiation of Subduction. Science 318 doi: 10.1126/1148494.

Hirajima T, Banno S, Hiroi Y and Ohta Y (1988) Phase petrology of eclogites and related rocks from the Motalafjella high-pressure metamorphic complex in Spitsbergen (Artic ocean) and its significance. Lithos 22: 75–97.

Honegger K, Le Fort P, Mascle G and Zimmermann JL (1989) The blueschists along the Indus Suture Zone in Ladakh, NW Himalaya. J Metamorph Geol 7: 57–72.

Hyndman RD (1995) The lithoprobe corridor across the Vancouver Island and tectonic consequences of subduction. Can J Earth Sci 32: 1777–1802.

Jahn B-M, Caby R and Monie P (2001) The oldest UHP eclogites of the world: age of UHP metamorphism, nature of protoliths and tectonic implications. Chem Geol 178: 143–158.

Jan MQ (1985) High-P rocks along the suture zone around Indo-Pakistan plate and phase chemistry of blueschists from eastern Ladakh. Geol Bull Univ Peshawar 18: 1–40.

Jolivet L, Faccenna C, Goffé B, Burov E and Agard P (2003) Subduction tectonics and exhumation of high-pressure metamorphic rocks in the Mediterranean orogens. Am J Sci 303: 353–409.

Jolivet L, Raimbourg H, Labrousse L, Avigad D, Leroy Y, Austrheim, H and Andersen TB (2005) Softening trigerred by eclogitization, the first step toward exhumation during continental subduction. Earth Planet Sci Lett 237: 532–547.

Kadarusman A, Massonne HJ, Van Roermund H, Permana H and Munasri A (2007) P-T evolution of eclogites and bleuschists from the Luk Ulo Complex of Central Java, Indonesia. Int Geol Rev 49: 329–356.

Kimura G, Mayurama S, Isozaki Y and Terabayashi Y (1996) Well-preserved underplating structure of the jadeitited Franciscan complex, Pacheco, California. Geology 24: 75–78.

Ko ZW, Enami M and Aoya M (2005) Chloritoid-bearing basic schists from the Sanbagawa metamorphic belt, central Shikoku: their petrologic significance and tectonic implications. J Mineral Petrol Sci 100: 43–54.

Krebs M, Maresh WM, Schertl HP, Baumann A, Draper G, Ildeman B, Münker C and Trapp E (2008) The dynamics of intra-oceanic subduction zones: a direct comparison between

fossil petrological evidence (Rio San Juan Complex, Dominican Republic) and numerical simulation. Lithos doi: 10.1016/J.lithos.20007.09.003.
Labrousse L, Jolivet L, Agard P, Hébert R and Andersen TB (2002) Crustal scale boudinage and migmatization of gneiss during their exhumation in the UHP province of Western Norway. Terra Nova 14: 263–270.
Lagabrielle Y and Polino R (1985) Origine volcano-détritique de certaines prasinites des schistes lustrés du Queyras (France): arguments texturaux et géochimiques. Bull Soc Geol France 4: 461–471.
Lagabrielle Y, Auzende JM, Cornen G, Juteau T, Lensch G, Mével C, Nicolas A, Prichard H, Ribeiro A and Vanney JR (1981) Observations par submersible de croûte océanique affleurant sur le banc de Corringe (SW Portugal): evidences de processus de démantellement des gabbros en milieu sous marin. C Acad Sci 293: 827–832.
Lallemand S (1999) La subduction océanique. Gordon and Bridge Science Publishers: 194p.
Lallemand S and Le Pichon X (1987) Coulomb wedge models applied to the subduction of seamounts in the Japan Trench. Geology 15: 1065–1069.
Lardeaux JM, Ledru P, Daniel I and Duchêne S (2001) The Varisan French Massif Central – a new addition to the Ultra-high pressure 'club': exhumation and geodynamic consequences. Tectonophysics 332: 143–167.
Le Pichon X, Henry P and Goffe B (1997) Uplift of Tibet: from eclogites to granulites: implication for the Andean Plateau and the Variscan Belt. Tectonophysics 273: 57–76.
Lee CT and Chen WP (2007) Possible density segregation of subducted oceanic lithosphere along a weak serpentinite layer and implications for compositional stratification of the Earth's mantle. Earth Planet Sci Lett 255: 357–366.
Leech ML, Singh S, Jain AK, Klemperer SL and Manickavasagam RM (2005) The onset of India-Asia continental collision: early, steep subduction required by timing of UHP metamorphism in the western Himalaya. Earth Planet Sci Lett 234: 83–97.
Liati A (2005) Identification of repeated Alpine UHP metamorphic events by U-Pb SHRIMP geochronology and REE geochemistry of zircon: the Rhodope zone of Northern Greece. Contrib Mineral Petrol 150: 608–630.
Li XP, Rahn M and Bucher K (2004) Serpentinites of the Zermatt-Saas ophiolite complex and their texture evolution. J Metam Geol 22: 159–177.
Liou JG (1990) HP minerals from deeply subducted metamorphic rocks. In Ultra-High Pressure Mineralogy, RJ Hemley ed, Rev Mineral 37: 33–96.
Liou JG, Hacker BR and Zhang RY (2000) Into the Forbidden Zone. Science 287: 1215–1216.
Liou JG, Tsujimori T, Zhang RY, Katayama I and Marayuma S (2004) Global UHP metamorphism and continental subduction/collision: the Himalayan model. Int Geol Rev 46: 1–27.
Liu F, Gerdes A, Liou JG, Xue HM and Liang FH (2006) SHRIMP U-Pb zircon dating from Sulu-Dabie dolomitic marble, eastern China: constraints on prograde, ultrahigh-pressure and retrograde metamorphic ages. J Metam Geol 24: 569–589.
Liu J, Bohlen SR and Ernst WG (1996) Stability of hydrous phases in subducting oceanic crust. Earth Planet Sci Lett 143: 161–171.
Lombardo B, Nervo R, Compagnoni R, Messiga B, Kienast JR, Mevel C, Fiora L, Piccardo G and Lanza R (1978) Osservazioni preliminari sulle ofioliti metamorfiche del monviso (Alpi occidentali). R Soc Ital Mineral Petrol 34: 253–305.
Maekawa H, Shozui M, Ishii T, Fryer P and Pearce JA (1993) Blueschist metamorphism in an active subduction zone. Nature 364: 520–523.
Mahéo G, Fayoux C, Guillot S, Garzanti E, Capiez P and Mascle G (2006) Geochemistry of ophiolitic rocks and blueschists from the Sapi-Shergol mélange (Ladakh, NW Himalaya, India): implication for the timing of the closure of the Neo-Tethys ocean. J Asia Earth Sci 26: 695–707.
Maruyama S, Liou JG and Terabayashi M (1996) Blueschists and eclogites of the world and their exhumation. Int Geol Rev 38: 485–594.
Massonne HJ (2003) A comparison of the evolution of diamondiferous quartz-rich rocks from the Saxonian Erzgebirge and the Kokchetav Massif: are so-called diamondiferous gneisses magmatic rocks? Earth Planet Sci Lett 216: 347–364.
Medaris G, Wang H, Jelínek E, Mihaljevic M and Jakeš P (2004) Characteristics and origins of diverse Variscan peridotites in the Gföhl Nappe, Bohemian Massif, Czech Republic. Lithos 82: 1–23.
Medaris LG (1999) Garnet peridotites in Eurasian high-pressure and ultrahigh pressure terranes: a diversity of origins and thermal histories. Inter Geol Rev 41: 799–815.
Messiga B, Kienast J-R, Rebay G, Riccardi MP and Tribuzio R (1999) Cr-rich magnesio-chloritoid eclogites from the Monviso ophiolites (Western Alps, Italy). J Metam Geol 17: 287–299.
Mével C (2003) Serpentinization of abyssal peridotites at mid-ocean ridges: Comptes Rendus Géoscience, 335: 825–852.
Michard A, Chopin C and Henry C (1993) Compression versus extension in the exhumation of the Dora-Maira coesite-bearing unit, Western Alps, Italy. Tectonophysics 221: 173–193.
Môller A, Appel P, Mezger K and Schenk V (1995) Evidence for a 2 Ga subduction zone; eclogites in the Usagaran Belt of Tanzania Andreas Moeller, Peter Appel, Klaus Mezger, and Volker Schenk: Geology 23: 1067–1070.
Monteleone BD, Baldwin SL, Webb LE, Fitzerald PG, Grov M and Schmitt AK (2007) Late Miocene-Pliocene eclogite facies metamorphism, D'Entrecasteaux islands, SE Papua New Guinea. J Metam Geol 25: 245–265.
Moore DE and Lockner D (2007) Comparative deformation bahavior of minerals in serpentinized ultramafic rocks: application to the slab-mantle interface in subduction zones. Inter Geol Rev 49: 401–415.
Moore JC and Silver EA (1987) Continental margin tectonics: submarine accretionary prisms. Rev Geophys 25: 1305–1312.
Moyen JF, Stevens G and Kisters A (2006) Record of mid-Archaean subduction from metamorphism in the Barberton terrain, South Africa. Nature 442: doi:10.1038/nature04972.
Negredo AM, Replumaz A, Villasenor A and Guillot S (2007) Modelling the evolution of continental subduction in the Pamir-indu Kush region. Earth Planet Sci Lett 259: 212–225.
Nimis P and Morten L (2000) P-T evolution of crustal garnet peridotites and included pyroxenites from Nonsberg area

(upper Austroalpine), NE Italy: from the wedge to the slab. J Geodyn 30: 93–115.
Nimis P and Trommsdorf V (2001) Revised Thermobarometry of Alpe Arami and other garnet peridotites from the Central Alps. J Petrol 42: 103–115.
O'Brien P, Zotov N, Law R, Khan AM and Jan MQ (2001) Coesite in Himalayan eclogite and implication for models of India-Asia collision. Geology 29: 435–438.
Och DJ, Leitc EC, Caprarelli G and Watanabe T (2003) Blueschist and eclogite in tectonic melange, Port Macquarie, New South Wales, Australia. Mineral Mag 67: 609–624.
Oh CW and Liou JG (1990) Metamorphic evolution of two different eclogites in the Franciscan Complex, California, USA. Lithos 24: 41–53.
Ota T, Terabayashi M and Katayama I (2004) Thermobaric structure and metamorphic evolution of the Iratsu eclogite body in the Sanbagawa belt, central Shikoku, Japan. Lithos 73: 95–126.
Palmeri R, Ghiribelli B, Ranalli G, Talrico F and Ricci A (2007) UHP metamorphism and exhumation of garnet-bearing ultramafic rocks from the Lanterman range (northern Victoria Land, Antarctica). J Metam Geol 25: 225–243.
Parkinson CD, Miyazali K, Wakita K, Barber AJ and Carswell DA (1998) An overview and tectonic synthesis of the pre-Tertiray very high-pressure metamorphic and associated rocks of Java, Suwalesi and Kalimantan, Indonesia. Isl Arc 7: 184–200.
Parra T, Vidal O and Jolivet L (2002) Relation between the intensity of deformation and retrogression in blueschist metapelites of Tinos Island (Greece) evidenced by chlorite-mica local equilibria. Lithos 63: 41–66.
Parrish R, Gough SJ, Searle M and Dave W (2006) Plate velocity exhumation of ultrahigh-pressure eclogites in the Pakistan Himalaya. Geology 34: 989–992.
Pawley AR (1994) The pressure and stability limits of lawsonite: implication for H_20 recycling in subduction zones. Contrib Mineral Petrol 118: 99–108.
Peacock SM and Wang K (1999) Seismic consequences of warm versus cool subduction zone metamorphism: examples from northeast and southwest Japan. Science 286: 937–939.
Perchuk A and Philippot P (1997) Rapid cooling and exhumation of eclogitic rocks from the Great Caucassus, Russia. J Metam Geol 15: 299–310.
Perraki M, Proyer A, Mposkos E, Kaindl R and Hoinkes G (2006) Raman micro-spectroscopy on diamond, graphite and other carbon polymorphs from the UHP metamorphic Kimi complex of the Rhodope Metamorphic province, NE Greece. Earth Planet Sci Lett 241: 672–685.
Philippot P and Kienast JR (1989) Chemical-microstructural changes in eclogite-facies shear zones (Monviso, Western Alps, north Italy) as indicators of strain history and the mechanism and scale of mass transfer. Lithos 23: 179–200.
Philippot P and Van Roermund HLM (1992) Deformation processes in eclogitic rocks: evidence for the rheological delamination of the oceanic crust in deeper levels of subduction zones. J Struct Geol 14: 1059–1077.
Philippot P, Blichert-Toft J, Perchuk A, Costa S and Gerasimov VY (2001) Lu–Hf and Ar–Ar chronometry supports extreme rate of subduction zone metamorphism deduced from geospeedometry. Tectonophysics 342: 23–38.
Platt J and Vissers RLM (1989) Extensional collapse of thickened continental lithosphere: a working hypothesis for the Alboran sea and Gibraltar arc. Geology 17: 540–543.
Platt JP (1986) Dynamic of orogenic wedges and the uplift of high-pressure metamorphic rocks. Geol Soc Am Bull 97: 1037–1053.
Platt JP (1987) The uplift of high-pressure low temperature metamorphic rocks. Phil Trans Roy Soc London A321: 87–103.
Ranero CR, Morgan JP, McIntsoh K and Reichert C (2003) Bending-related faulting and mantle serpentinization at the Middle America trench. Nature 425: 367–373.
Reinecke T (1991) Very-high pressure metamorphism and uplift of coesite-bearing metasediments from the Zermatt-Saas zone, Western Alps. Eur J Mineral 3: 7–17.
Reynard B, Hilairet N, Balan E and Lazzeri M (2007) Elasticity of serpentines and extensive serpentinization in subduction zones. Geophys Res Lett 34: doi:10.1029/2007GL030176.
Root DB, Hacker BR, Gans PB, Ducea MN, Eide EA and Mosenfelder JL (2005) Discrete ultrahigh-pressure domains in the western Gneiss Region, Norway: implications for formation and exhumation. J Metam Geol 23: 45–61.
Rubatto D and Hermann J (2001) Exhumation as fast as subduction? Geology 29: 3–6.
Saumur BM, Hattori KH and Guillot S (2007) Protrusion of fore-arc mantle serpentinites together with HP and UHP rocks along major strike-slip faults in the northern subduction complex of Dominican Republic. Subduction zone geodynamics Conference, Montpellier.
Schmidt MW and Poli S (1998) Experimentally based water budgets for dehydrating slabs and consequences for arc magma generation: Earth and Planetary Science Letters 163: 361–379.
Schneider J, Bosch D, Monié P, Guillot S, Garcia-Casco AG, Lardeaux JM, Torres-Roldan RL and Millan T (2004) Origin and evolution of the Escambray massif (Central Cuba): an example of HP/LT rocks exhumed during intraoceanic subduction. J Metamorph Geol 22: 227–247.
Schwartz S, Lardeaux JM, Guillot S and Tricart P (2000) Diversité du métamorphisme éclogitique dans le massif ophiolitique du Monviso (Alpes Occidentales, Italie). Geodinam Acta 13: 169–188.
Schwartz S, Allemand P and Guillot S (2001) Numerical model of the effect of serpentinites on the exhumation of eclogitic rocks: insights from the Monviso ophiolitic massif (western Alps). Tectonophysics 42: 193–206.
Schwartz S, Lardeaux JM, Tricart P, Guillot S and Labrin E (2007) Diachronous exhumation of subducted HP metamorphic rocks from southwestern Alps: evidences from fission-track analysis. Terra Nova 19: 133–140.
Searle M, Hacker BR and Bilham R (2001) The Hindu Kush seismic zone as a paradigm for the creation of ultrahigh pressure diamond- and coesite- bearing continental rocks. J Geol 109: 143–53.
Seno T and Yamasaki T (2003) Low frequency tremors, intraslab and interplate earthquakes in southwest Japan, from a viewpoint of slab dehydration. Geophys Res Lett 30: 22 2171- doi 10.1029/2003GLO18349.
Shreve RL and Cloos M (1986) Dynamics of sediment subduction, melange formation and prism accretion. J Geophys Res 91: 10 229–10 245.

Smith DC (1984) Coesite in clinopyroxene in the Caledonides and its implication for geodynamics. Nature 310: 641–644.

Sobolev SV and Shatsky VS (1990) Diamond inclusions in garnets from metamorphic rocks: a new environment for diamond formation. Nature 343: 742–746.

Sorensen SS (1988) Petrology of amphibolite-facies mafic and ultramafic rocks from the Catalina Schist, southern California: metasomatism and migmatization in a subduction zone metamorphic setting. J Metam Geol, 6, doi:10.1111/j.1525-1314.1988.tb00431.x: 405–435.

Spengler D, Van Roermund H, Drury MR, Ottolini L, Mason PRD and Davies GF (2006) Derep origin and hot melting of an Archean orogenic peridotite massif in Norway. Nature 440: 913–917.

Stanek KP, Maresch WV, Grafe F, Grevel CH and Baumann A (2006) Structure, tectonics and metamorphic development of the Sancti Spiritus Dome (eastern Escambray massif, Central Cuba). Geol Acta 4: 151–170.

Steck A, Epard JL, Vannay JC, Hunziker J, Girard M, Moraro A and Robyr M (1998) Geological transect across the Tso Moarari and Spiti areas: the nappe structures of the Tethys Himalaya. Eclo Geol Helv 91: 103–121.

Stöcker B and Gerya TV (2005) Pre-collisional HP metamorphism and nappe tectonics at active continental margins: a numerical simulation. Terra Nova doi10.1111/j.1365-3112.2004.00589.

Stöckert B and Renner J (1998) Rheology of crustal rocks at ultrahigh pressure. In: Hacker BR and Liou JG (eds) When continent collide: Geodynamics and Geochemistry of Ultrahigh-pressure rocks, Kuwer Academic Publishers, Dordrecht: 57–95.

Terry MP Robinson P and Ravna EJK (2000) Kyanite eclogite thermobarometry and evidence for thrusting of UHP over HP metamorphic rocks, Nordoyane, Western Gneiss Region, Norway: American Mineralogist 85: 1637–1650.

Thompson A, Schulmann K and Jezek J (1997) Extrusion tectonics and elevation of lower crustal metamorphic rocks on convergent orogens. Geology 25: 491–494.

Treloar PJ, O'Brian PJ, Parrish RR and Khan AM (2003) Exhumation of early Tertiary, coesite-bearing eclogites from the Pakistan Himalaya. J Geol Soc London 160: 367–376.

Tricart P and Schwartz S (2007) A north-south section across the Queyras Schistes Lustrés (Piedmont zone, Western Alps): Syn-collision refolding of a subduction wedge. Eclogae Geol Helv 99 Doi 10.1007/s00015-006-1197-6.

Tricart P, Schwartz S, Sue C and Lardeaux JM (2004) Evidence for synextensional tilting and doming during during final exhumation from analysis multistage faults (Queyras, Schsites Lustrés, Western Alps). J Struct Geol 26: 1633–1645.

Tsujimori T, Sisson VB, Liou JG, Harlow GE and Sorensen SS (2006) Very-low-temperature record of the subduction processes: a review of worldwide lawsonite eclogites. Lithos 92: 609–624.

Tucker RD, Krogh TE and Rahei A (1991) Proterozic evolution and age province boundaries in the central part of the Western Gneiss Region: results of U-Pb dating of accessory minerals from Trondheimsford to Geiranger. In: Gower CF, Rivers R and Ryan B (eds) Mid-Proterozic laurentia Baltica. Geol Soc Spe Paper 38: 149–173.

Ueda H, Usuki T and Kuramoto Y (2004) Intraoceanic unroofing of eclogite facies rocks in the Omachi Seamount, Izu-Bonin frontal arc. Geology 32: 849–852.

Ulmer P and Trommsdorff V (1995) Serpentinite stability to mantle depths and subduction related magmatism. Science 268: 858–861.

Valli F, Guillot S and Hatori K (2004) Source and tectono-metamorphic evolution of mafic and pelitic metasedimentary rocks from the central Quetico metasedimentary belt, Archean Superior, Province of Canada. Precam Res 132: 155–177.

Van der Beuckel J (1992) Some thermo-mechanical aspects of the subduction of continental lithosphere. Tectonics 11: 316–329.

Van Roermund HLM, Drury MR, Barnhoorn A and de Ronde A (2001) Relict majoritic garnet microstructures from ultra-deep orogenic peridotites in Western Norway. J Petrol 42: 117–130.

Vaugh R and Parkinson D (2003) Comparison and tectonic significance of Pan-African HP/UHP eclogites from Pernambuco and Minas Gerais, Brazil. Geol Soc Am Abst Prog 35: 632.

Vignaroli G, Rossetti F, Bouybaouene M, Massonne HF, Theye T and Faccenna C (2005) A counter-clockwise P-T path for the Voltri massif eclogites (Ligurian Alps, Italy). J Metamorph Geol 23: doi:10/1111/j.152561314.2005.00592.

Von Huene R and Cullota R (1989) Tectonic erosion at the front of the Japan trench convergent margin. Tectonophysics 160: 75–90.

Von Huene R and Scholl D (1991) Observations at convergent margins concerning sediment subduction, subduction erosion, and the growth of continental crust. Rev Geophys 29: 279–316.

Wallis S, Moriyama Y and Tagam T (2004) Exhumation rates and age of metamorphism in the Sanbagawa belt: new constraints from zircon fission track analysis. J Metam Geol 22: 17–24.

Willner AP, Glodny J, Gerya TV, Godoy E and Massonne A (2004) A counterclockwise PTt-path of high pressure-low temperature rocks from the coastal Cordillera accretionary complex of South Central Chile: constraints for the earliest stage of subduction mass flow. Lithos 75: 283–310.

Yamasaki T and Seno T (2003) Double seismic zone and dehydration embrittlement of the subducting slab J Geophys Res 108: B4, 2212, doi: 101029/2002JB001918.

Yang JS, Xu Z, Dobrzhinetskaya LF, Green HW, Pei X, Shi R, Wu C, Wooden JL, Zhang JS, Wan Y and Li H (2003) Discovery of metamorphic diamonds in central China: an indication of a >4000-km-long zone of deep subduction resulting from multiple continental collisions. Terra Nova 15: 370–379.

Yang JS, Dobrzhinetskaya L, Bai WJ, Fanq QS, Robinson PT, Zhang, J and Green II HW (2007) Diamond- and coesite-bearing chromitites from the Luobusa ophiolite, Tibet Geology, 35, doi: 10.1130/G23766A.1.

Young DY, Hacker BR, Andersen TB and Corfu F (2007) Prograde amphibolite facies to ultrahigh-pressure transition from Nordfjord, western Norway: implications for exhumation tectonics. Tectonics 26: doi:10.1029/2004TC001781.

Yamato P, Agard P, Burov E, Le Pourhiet L, Jolivet L and Tiberi C (2007) Burial and exhumation in a subduction wedge: mutual constraints from thermomechanical and natural P-T-t data (Schistes Lustrés, western Alps). J Geophys Res 112: B07410, doi: 10.1029/2006JB004441.

Zack T, Rivers T, Brumm R and Kronz A (2004) Cold subduction of oceanic crust: implications from a lawsonite eclogite from the Dominican Republic. Eur J Mineral 16: 909–916.

Zhang L, Ellis DJ, Arculus RJ, Jiang W and Wei CJ (2003) Forbidden zone subduction of sediments to 150 km depth-the reaction of dolomiye + aragonite in the UHPM metapelites from western Tiansjhan, China. J Metam Geol 21: 523–529.

Zhang RY, Liou JG, Yang JS and Yui T-F (2000) Petrochemical constraints for dual origin of garnet peridotites from the Dabie-Sulu UHP terrane, eastern-central China. J Metam Geol 18: 149–166.

Zhao ZY, Wei CJ and Fang AM (2005) Plastic flow of coesite in a deep continental subduction regime: microstructures, deformation mechanisms and rheological implications. Earth Planet Sci Lett 237: 209–222.